The Hong Kong Polytechnic University

Department of Electronic and Information Engineering

Development of Driver and Color Control System for High-Power RGB LED

Ng Sau Kin, Nick

A thesis submitted in partial fulfillment of the

requirements for the degree of

Master of Philosophy

October 2012

CERTIFICATE OF ORIGINALITY

I hereby declare that this thesis is my own work and that, to the best of my knowledge and belief, it reproduces no material previously published or written, nor material that has been accepted for the award of any other degree or diploma, except where due acknowledgement has been made in the text.

_____ (Signed)

Ng Sau Kin (Name of Student)

To my family

Abstract

A bilevel driving approach was proposed in the literature for mitigating the energy wastage associated with driving LEDs at high peak current. The main idea is to introduce two drive parameters, i.e., high/low PWM current levels and duty cycles, that give rise to a 2-D luminosity control capability. The same idea was later generalized to an n-level driving approach for maximizing the electrical-to-light conversion efficiency of LEDs. Although previous uses of the n-level driving approach have been focusing on improving the luminous efficacy of LEDs, it is shown in this thesis that its 2-D luminosity control feature can also lead to a significant improvement in color resolution when applied to driving RGB LEDs, hence making it well suited for applications in large-area LED display panels. In comparison to the first prototype driver proposed by the inventor of the driving approach, a more practical implementation of the complex 2-D driving approach with digital microcontroller is demonstrated. The various technical aspects of the driving approach, including luminous efficacy, color resolution, and color stability over dimming, are discussed in this thesis with the aid of experimental results.

This thesis also presents a method of controlling the white color point in red/green /blue (RGB) LED driver system. In contrast to conventional systems where the average driving currents of the primary-color LEDs can become saturated when the LEDs have sufficiently aged, and causes the resulting white color point to go out of regulation, the proposed method avoids this problem by adjusting the color set points when a pre-defined threshold current is reached by one or more of the primary-color LEDs. It is shown that the method can effectively maintain the white color point of the RGB LED at the desired value when the LEDs are subjected to an accelerated ageing through repetitive current stress cycles.

Publications

Journal Papers

1. Ng, S. K.; Loo, K. H.; Ip, S. K.; Lai, Y. M.; Tse, C. K.; Mok, K. T.; , "Sequential Variable Bilevel Driving Approach Suitable for Use in High-Color-Precision LED Display Panels," IEEE Transactions on Industrial Electronics, vol.59, no.12, pp.4637-4645, Dec. 2012

2. Ng, S. K.; Loo, K. H.; Lai, Y. M.; Tse, C. K.; , "Color Control System for RGB LED with Application to Light Sources Suffering from Prolonged Ageing," IEEE Transactions on Industrial Electronics , Oct. 2012 (submitted)

Conference Papers

1. Ng, S.K.; Loo, K.H.; Lai, Y.M.; Mok, K.T.; Tse, C.K.; , "Variable bi-level phase-shifted driving method for high-power RGB LED lamps," Power Electronics and ECCE Asia (ICPE & ECCE), 2011 IEEE 8th International Conference on , vol., no., pp.782-787, May 30 2011-June 3 2011

2. Ng, S.K.; Loo, K.H.; Lai, Y.M.; Tse, C.K.; , "Color Control in RGB Driver System Applicable to LED of All Ageing Conditions", IECON2012, Montreal, Canada

Acknowledgments

I would like to express my gratitude to my chief supervisor Dr. Y. M. Lai for his patience, consistent guideline and unlimited support on the research during the course of my MPhil study. He has broadened my knowledge and strengthened my engineering sense. Also, I would like to thank my co-supervisor, Dr. K. H. Loo, he has offered me plenty of guidance. I have overcome various technical problems on my road of research and I have learnt many analytical skills from him.

Besides, I wish to thank Prof. C. K. Michael Tse. He has offered me the chance to work in his group, where I have earned invaluable learning experiences and exposures. In addition, I would like to extend my gratitudes to the members of the Applied Nonlinear Circuits and Systems Research Group as well as other members of the department who gave me all kinds of supports. They have offered me numerous assistances and valuable comments in my study. In particular, they are S. Y. Lam, Barry Mok, Sitthisak Kiratipongvoot, Kit Cheung, Richard Wong, K.C. Tsang, Martin Cheung, Cao Ling Ling, Luo Fei and Shen Zhenyu . I will never forget the memorable days and joyful experiences working with them.

Last but not least, I must thank my family and Ching for their loves, cares and understandings. They gave me immense support in my study.

Table of Contents

List of Figures

List of Tables

Chapter 1

Introduction

1 Background

Lighting contributes to 20 % of our electricity consumption. If incandescent lamps are used as light source, 90 % of the electrical power consumed is converted to heat due to their low efficacy. The efficacy of incandescent lamps are about 20 lm/W and its life time is only 2,000 hours. They were our first electrical light source invented by Swan and Edison in 1879.

Before the invention of campact fluorescent lamp(CFL), a mercury discharge lamps were invented by the General Electric (GE) Company in 1938, they offer an efficacy up to 80 lm/W and a life time up to 15,000 hours. However, their efficacy remained at a plateau without much breakthrough for the last ten years. Besides, they contain mercury vapor and emit UV light during their operation. Their glass body is fragile which makes them non-robust.

High brightness light-emitting diodes (HB LED) has become popular as they offer many attractive features. The efficacy of HB LED has reached over 208 lm/W which is ten times that of incandescent lamps and more than twice that of the CFLs

[6]. Unlike CFLs, LEDs do not contain poisonous mercury vapor, do not emit UV light during their operation, exhibit fast electric-to-light response, robust, compact and long life time (up to 100,000 hours).

In 1907, the first electroluminescence was demonstrated by H.J. Round at the Marconi Lab, who discovered the phenomenon of light emission from a silicon carbide (SiC) crystal. Since 1962, the earliest red LED device was based on GaAsP alloy developed by Nick Holonyak Jr. at the GE Company [7]. However, the light output efficiency was very low and not sufficient for use in general lighting. An AllnGaP/GaP-based red LED was reported in 1990, the output efficiency was ten times higher than incandescent lamp [8]. However, the production white light requires the combination of red, green and blue light but the green and blue LEDs were not available.In 1994, the first blue LED and green LED based on InGaN alloy were invented by Nakamura [9]. In 1996, the first high-brightness white LED, based on blue LED coated with yellow phosphor was developed by Nakamura at Nichia.

1.1 LED Basics

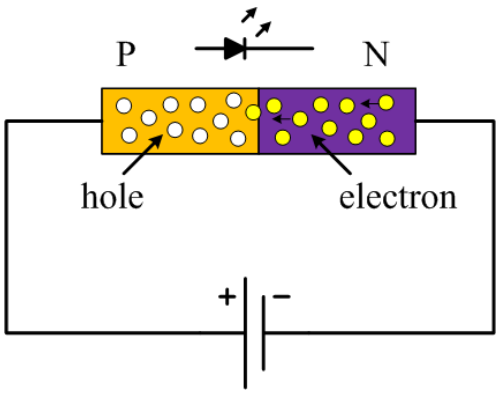

Figure 1-1: Simplified LED circuit driving a P-N junction.

The structure of an LED is similar to a P-N juntion having an I-V characteristic

resembling a diode. When a forward bias voltage is applied to a p-n junction, electrons flow from the cathode to anode (shown on Fig. (1-1)). When majority electrons meet with minority holes, or vice versa, they recombine and release energy equal to the semiconductor's band gap energy in the form of photon. The wavelength of the emitted photons depends on the properties of the semiconductor used. Aluminium gallium arsenide (AlGaAs) or aluminium indium gallium phosphide (AlInGaP) produce red LED, while indium gallium nitride (InGaN) and its varied compositions produce green and blue LEDs. White LEDs are produced by coating blue LED with yellow phosphor (YAG) [10, 11].

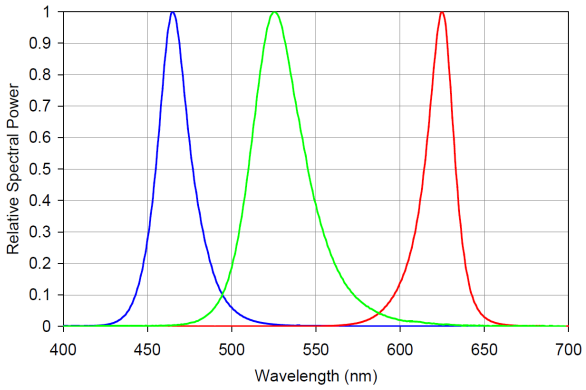

Figure 1-2: Color spectrum of RGB LED [1].

Fig. 1-2 shows the spectrum of a RGB LED.The dominate wavelength of blue LED is in the range of 450 to 500 nm, followed by the green LED in between the range of 500 to 590 nm and the red LED in the range of 610 to 760 nm. The Full Wave Half Maximum (FWHM) spectral bandwidth of these primary colors is approximately 24-27 nm. Theoretically,when these primary colors are combined, any color on the CIE color space including the white color point can be produced.

Optical Characteristic

One major figure of merit of LED is efficacy. Typically, the unit of luminous flux , lumen $(\mathrm{lm\ or\ cd \cdot sr})$, is used to describe the intensity of a light source as perceived by human eyes, and its definition is given by Eqn. (1.1). The standard luminosity function is normalized to a peak value of unity at 555 nm (green light peak wavelength). The value of the constant in front of the integral is usually rounded off to 683 lm/W, where $\mathrm{V}(\lambda)$ is the weighted sensitivity function of human eyes and $\mathrm{P}(\lambda)$is the spectral power density.

$$\Phi = 683 \int_{\lambda} V(\lambda) P(\lambda) d\lambda \tag{1.1}$$

From Eqn.(1.1), the light efficacy is defined as the ratio between the luminous flux and the emitted optical power:

$$\frac{\Phi}{P} = \frac{683 \int_{\lambda} V(\lambda) P(\lambda) d\lambda}{\int_{\lambda} P(\lambda) d\lambda} \tag{1.2}$$

Another important performance index for LED is the wall-plug efficiency, η_w, which is defined as the ratio of luminous flux to the electrical input power of the LED. This parameter decreases with increasing heat sink temperature.

$$\eta_w = \frac{\Phi}{IV} \tag{1.3}$$

Generally, the luminous flux of LED increases nonlinearly with increasing forward current due to the droop effect [12]. LEDs made from different semiconductor material show different lumious flux behavior (Fig. 1-4). The luminous flux of LEDs also depends on their junction temperature (Fig. 1-3).

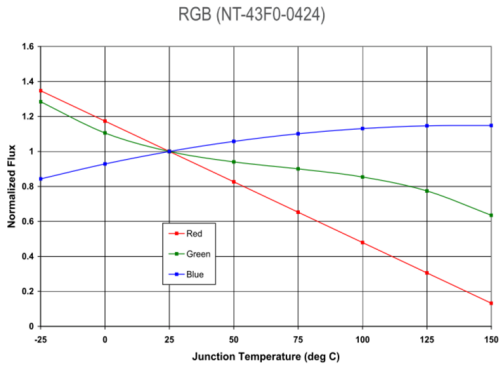

Figure 1-3: Output flux of RGB LED vs junction temperature [1].

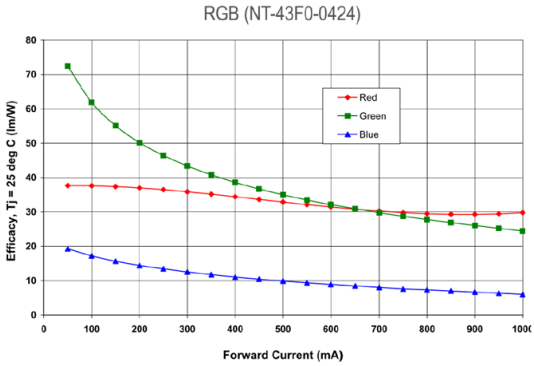

Figure 1-4: Output flux of RGB LED vs DC current [1].

Unlike incandescent lamps or CFLs, Which can fail abruptly due to broken lamp filaments, the lifetime of HB LED is more commonly characterized by a degradation of luminous flux over time. Normally, the time to failure of HB LED is measured in terms of L70 and L50, Which represent the time at which 70% and 50% of the initial luminous flux is attained.

Performance Indices for LED

There are serval important indexes which aim to describe the colored light source (including white light). The first color matching experiment was developed by Hermann Grabmann at around 1853. This was an experiment that used three linearly

independent spectra lamps mixing together in order to generate different colors. It was found out that for some conditions, some specific color contains one or even two negative values in the set of RGB combination (Fig. 1-5), called “negative” color. The amount of each primary color present in a light having a spectral power density $\mathrm{P}(\lambda)$ can be found by weighting it with the respective color-matching function and integrating the product over the visible range of wavelength:

$$
\begin{aligned}
R &= \int_{\lambda} \overline{r}(\lambda) P(\lambda) d\lambda \\
G &= \int_{\lambda} \overline{g}(\lambda) P(\lambda) d\lambda \\
B &= \int_{\lambda} \overline{b}(\lambda) P(\lambda) d\lambda
\end{aligned}
\tag{1.4}
$$

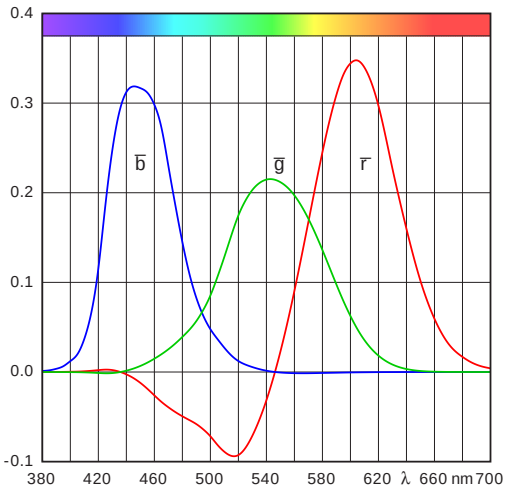

Figure 1-5: Normalized RGB color matching functions [2].

CIE 1931 specifies a color space that does not have negative color. Based on the new color-matching functions $(\overline{\mathrm{x}}(\lambda),\ \overline{\mathrm{y}}(\lambda)\ \mathrm{and}\ \overline{\mathrm{z}}(\lambda))$, the new tristimulus values X, Y and Z can be obtained from R,G,B using Eqn. (1.6), and vice versa using Eqn.

(1.7) [13].

$$X = \int_{\lambda} \overline{x}(\lambda)P(\lambda)d\lambda$$
$$Y = \int_{\lambda} \overline{y}(\lambda)P(\lambda)d\lambda \tag{1.5}$$
$$Z = \int_{\lambda} \overline{z}(\lambda)P(\lambda)d\lambda$$

$$\begin{bmatrix} X \\ Y \\ Z \end{bmatrix} = \begin{bmatrix} 0.57667 & 0.18556 & 0.18823 \\ 0.29734 & 0.62736 & 0.07529 \\ 0.02703 & 0.07069 & 0.99134 \end{bmatrix} \begin{bmatrix} R \\ G \\ B \end{bmatrix} \tag{1.6}$$

$$\begin{bmatrix} R \\ G \\ B \end{bmatrix} = \begin{bmatrix} 2.04159 & -0.56501 & -0.34473 \\ -0.96924 & 1.87597 & 0.04156 \\ 0.01344 & -0.11836 & 1.01517 \end{bmatrix} \begin{bmatrix} X \\ Y \\ Z \end{bmatrix} \tag{1.7}$$

$$u' = \frac{4X}{X + 15Y + 3Z}$$
$$v' = \frac{9Y}{X + 15Y + 3Z} \tag{1.8}$$

The chromaticity coordinates (u', v') can be calculated by Eq. (1.8). One of the most frequently used CIE color space is the CIE 1976 (CIELUV) chromaticity coordinate system. Typically, different ratio of RGB color intensity can generate any color inside the area of triangle in Fig. 1-6. This triangle is defined as the color gamut. The degree of color deviation from a reference color point can be calculated using Eqn. (1.9). Normally, a color deviation of $\Delta u'v' < 0.005$ is undetectable by human eyes.

$$\Delta u'v' = \sqrt{(u' - u'_o)^2 + (v' - v'_o)^2} \tag{1.9}$$

The Color Rendering Index (CRI) is another important performance index for

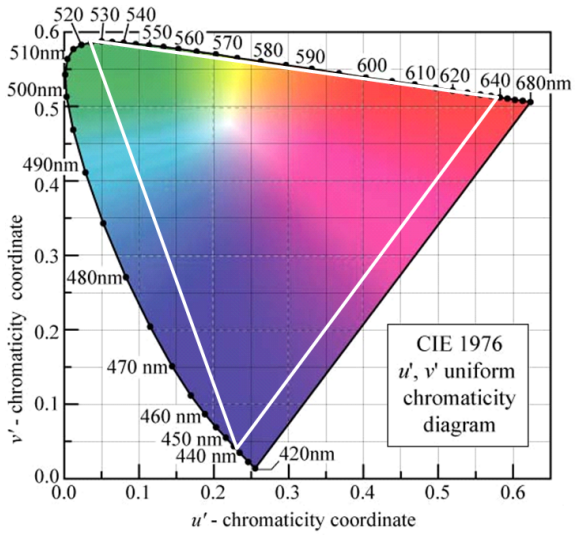

Figure 1-6: CIE 1976 color space.

indicating the color-rendering ability of a white light source relative to the sun light, and is measure in 0 to 100. Incandescent lamp has a CRI of 100 which is the closest to the sun light.Correlated Color Temperature (CCT) describes the temperature of a Planckian light source that has the same color property as the light source of interest. A lower CCT gives a warmer sensation, and a higher CCT gives a colder sensation. The CCT of standard natural sunlight is 6500K (D65) and the warmer one is 5000K (D50).

1.2 Applications

HB LEDs have been widely used in various applications, for example, white LED lamp for general and automotive lighting that have less stringent color requirement. For more color critical applications , RGB LEDs are used, such as the backlight of LCD display panels, projectors, and mobiles phones. RGB LEDs also find widespread application in large-area video display panels such as LED dot matrix panels in shopping malls or stadiums.

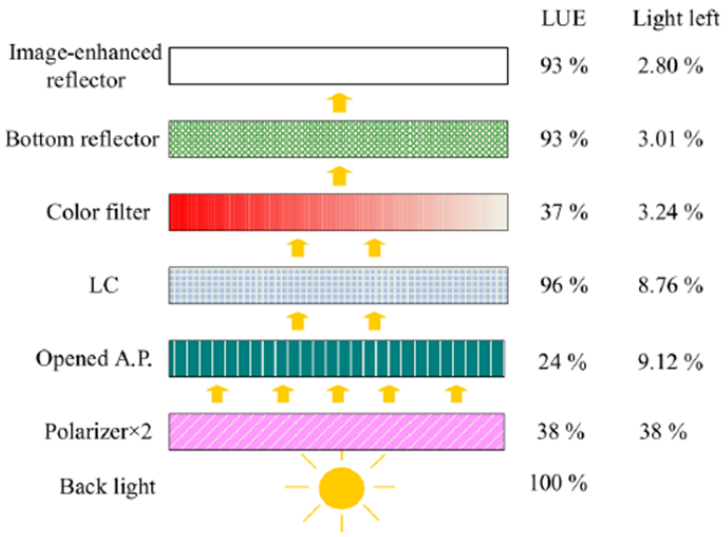

Figure 1-7: A block diagram of LCD' structure with backlight source and color filter [3].

Conventionally, the light sources used for a LCD display backlight are white LED or CFL. However, it was found that the CCT of these light sources are not easy to control to meet the standard particularly after they have been sufficiently aged. They also require additional components such as color filter to filter out unwanted color (see Fig. 1-7), and this consumes some of the emitted light, hence giving rise to poorer efficacy. In addition, the size of their color gamut is smaller than the standard (i.e. NTSC) due to the color filtering effect. This problem is remedied by the usage of RGB LED since color filters are removed [3, 14], and the overall power consumption is reduced. The typical power consumption of a 15.4-inch computer notebook's backlight using CCFL is 5 W while a color filter-less RGB backlight consumes $2 \sim 3$ W which represents a 50 % improvement [6]. Besides, another important usage of LCD backlight is the local dimming technique which controls the local intensity of the backlight according to the image to be displayed in order to enhance the contrast ratio [15]. This implies power consumption can be further reduced.

Apart from LCD display panels, the implementation of RGB LED backlight in video projectors is also gaining in popularity. Traditionally, the structure of a projector's lighting system is similar to that of the LCD display panel. Fig. 1-8 shows a traditional video projector system, where a light source at back of the transmissive LCD emits light passes through the lens and helps projecting the image onto the screen. Traditionally, incandescent lamps are used as the light source. However, their life time is relatively short (2,000 hours), the CCT is not satisfactory (not close to day light D65) and are very low in efficacy. They require color filtering prism for extracting desired color. Although the implementation using white LED helps to extend the life time of light source to around 50K hours, but using the color filter still blocks part of the emitted white light, and hence lower the system's efficiency. Therefore, using HB RGB LEDs is more superior compared to white LEDs or incandescent lamps.

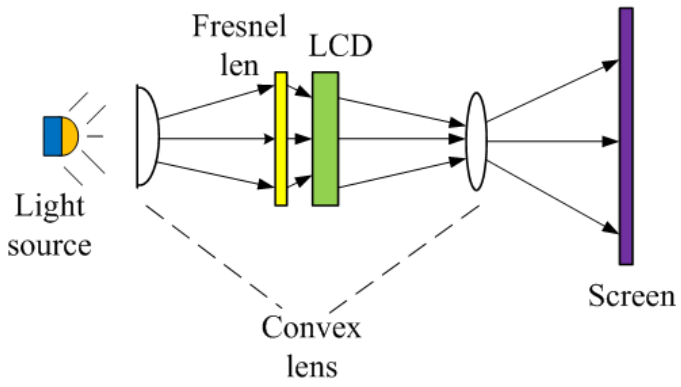

Figure 1-8: A block diagram of typical projection system.

The trend of the electronic world is to produce compact and portable products. Generally, the size of projectors is bulky due to the weight, size of the optical lens system and LCD, which degrade their portability. The recent invention of pico digital light projector (DLP) makes projectors portable. This optical technology makes use of the reflectance of a small mirror array on a chip, a structure known as the digital

micro-mirror device (DMD), instead of LCD (Fig. 1-9(a) and 1-9(b)). Using this technique, the size of pico-DLP can be small enough and can be embedded as a part of a mobile phone [16]. This is convenient for some applications that do not require high luminosity and high contrast ratio. Since the space inside the DLP is limited, the number of LEDs and the size of driving and controller circuitry are limited. Therefore, high efficacy and compact size of the internal lighting system is one of the main challenges in research on portable projectors.

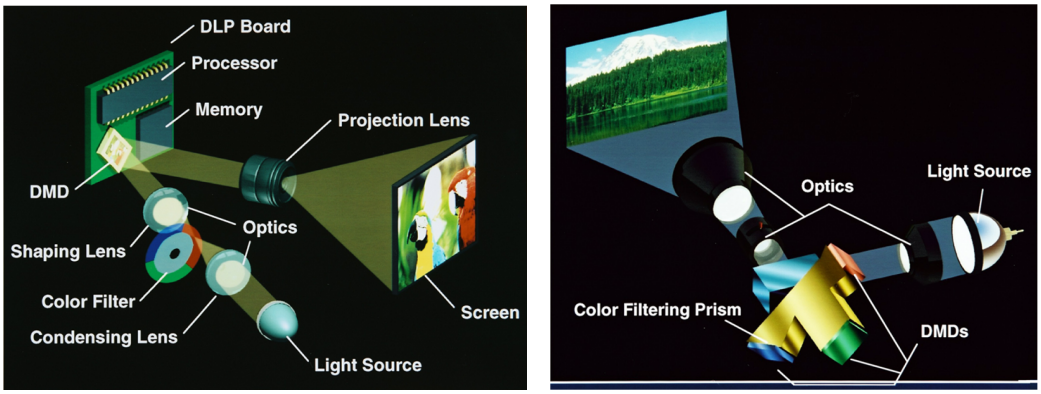

(a) One chip pico DLP with a color filter wheel. (b) Three chips pico-DLP with three prisms.

Figure 1-9: A structure of portable DLP [4].

2 Literature Review

The literature review is divided into three parts. The first part describes the properties of RGB LEDs and their performance under ageing and some methods for performing accelerated ageing test. The second part focuses on the details of different driving methods. The final part presents the currently available techniques for controlling the color stability of HB RGB LEDs.

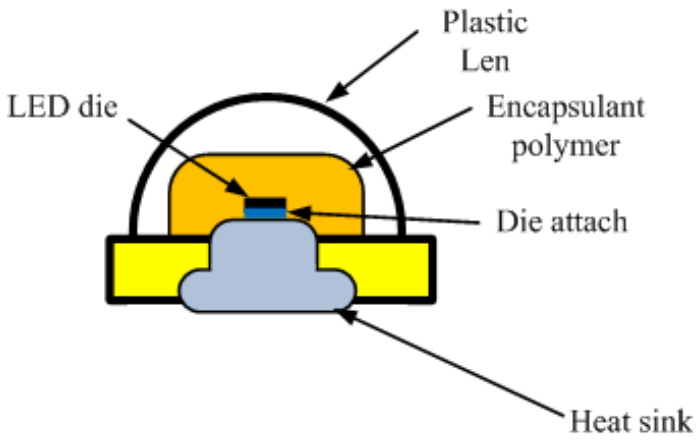

Figure 1-10: Simplified LED package structure.

2.1 Overview of RGB LED and their Ageing Characteristics

The structure of LED including its package is illustrated in Fig. 1-10. The LED die is attached at the center of the package on a heat sink. The die is surrounded with polymer resin such as epoxy or silicon resin [17, 18]. Finally a transparent plastic len covers the LED allowing light passing through it with a desired view angle.

Conventionally, the ageing process of LED is very slow, we need to use some methods for accelerating the ageing process in order to study the ageing mechanism with a reasonable time scale. There are two methods for accelerating this ageing process of LED: high DC current stress and high temperature stress. The method of high DC current stress is simple with the application of a high forward current density on the LED. This method is a easy and effective, but the drawback is that it will change the I-V characteristic rapidly and the ageing process can be easily ”over” accelerated. Furthermore, this method cannot provide observations on the change of other properties than the I-V characteristics, such as the browning of the epoxy resin lens. Unlike the DC current stress method, another method is high temperature stress with the LED housed in an oven controlled at a constant temperature and even humid-

ity. Typically, there is no standard prescribed to this test. However, there are some common temperatures used by LED researchers, such as $60^{\circ}\mathrm{C},\ 85^{\circ}\mathrm{C}$ and $200^{\circ}\mathrm{C}$ under $85\ \%$ humidity. For investigation of the browning process, the oven temperature should be more than $95^{\circ}\mathrm{C}$ as suggested by Tsai *et al.* [19].

$$I = I_S(\exp(\frac{eV}{nkT}) - 1) \tag{1.10}$$

The current-voltage (I-V) characteristic of LED is described by Eqn. (1.10), where I_S is the diodes reverse saturation current, n is the ideality factor, k is Boltzmanns constant and T is junction temperature of the LED in Kelvin scale. Clearly, the relationship between its current and voltage is non-linear. Besides, both the variations of junction temperature and ideality factor will affect the I-V characteristic [20]. For different color of LED, the effect of junction temperature is different to the optical performance. The ideality factor can vary depending on the quality of the PN junction and band gap energy. It can also vary during the ageing process [21].

The optical performance depends on several factors, including the electrical input power, junction temperature and the quality of medium through which the emitted light propagates (which are silicon resin or epoxy resin). All of these factors can vary with time, and which may cause the degradation of the optical performance of LED (including color variation), and associated with the ageing of LED. Increasing junction temperature not only causes the spectrum to shift to longer wavelength, which is known as red shift[22], but also accelerates the ageing process. On the other hand, the increased DC current causes the spectrum to shift to shorter wavelength, which is known as blue shift and also accelerates the aging process. The degree of wavelength shift depends on the composition of band gap material. Some of them is heavily affected by junction temperature, such as the materials used for making

red LED, AlGaAs, while other materials (such as GaN or InGaN to produce green and bule LED) are less affected by it. However, GaN- and InGaN-based LEDs are more sensitive to DC current change. There will be no color variation if the rate of wavelength change of red, green and blue LEDs are identical. Unfortunately, this is not the case in practice. Besides, there is another reason that can cause wavelength shift: the ageing process. The transparent epoxy in LED will yellow over time, and this yellowed lens actually alters the transmission of light at different wavelengths [19, 20, 18, 23].In general, the transmission of shorter wavelengths are lower than the longer ones which constitutes the reason for different ageing rates for LED emitting different wavelengths.

Apart from the yellowing lens, there are other property changes due to ageing that can lead to the degradation of optical performance. Buso *et al.* [24] and Meneghesso *et al.* [20] reported that the degradation of those GaN-based LEDs are mainly related to four kinds of property change. They are (I) increase of reverse leakage current; (II) increase of the generation-recombination current at low forward bias; (III) increase of ideality factor; and (IV) increase of the parasitic series resistance. However, Moon *et al.* [5] suggested that there is no direct relation between the degradation of optical performance and the increase of reverse leakage current or the increase of generation-recombination current. They agree only on the optical performance degradation due to significant increment in parasitic series resistance. Both high temperature and high DC current stress tests showed that the increment of parasitic resistance lead to lower optical output. The reason of increased parasitic resistance can be due to the degradation of the quality of semi-transparent ohmic contact and the top surface of p-GaN layer. Other possible reason are the decomposition of Mg complexes and Mg reactivation in the Mg mixed InGaN / GaN material, and the current crowding

effect [5]. The aforementioned four types of ageing characteristics are illustrated on Fig.1-11.

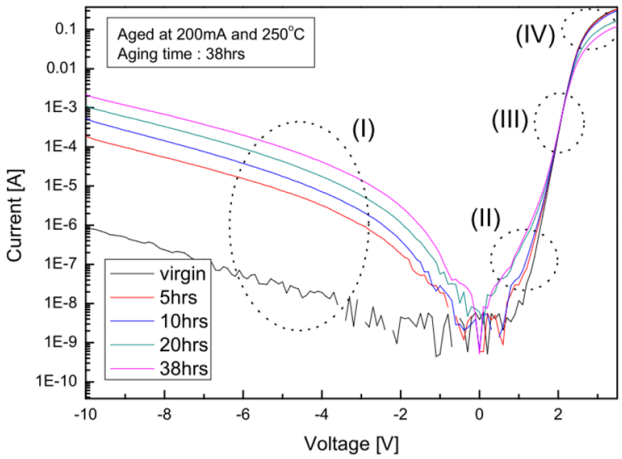

Figure 1-11: I-V characteristic after DC stress [5].

Furthermore, the inter-connection between the LED die and the embedded heat sink (as Fig. 1-10) , die attach, will tend to degrade during the long-term operation in a high temperature environment due to the high junction temperature of the LED [25]. In terms of thermal conduction path, a lower quality of the die attach may cause the junction-to-case thermal resistance to increase.

The red LED is mainly made by AlGaAs or AlInGaP compound semi-conductor materials. These materials are sensitive to temperature changes and their I-V characteristics are different for the GaN/InGaN based materials.

2.2 Overview of Driving Techniques

2.3 Driving Systems for RGB LEDs

For driving LEDs, switching mode power converters are preferred due to their hight efficiency. By using appropriate topologies, current driving technique and cascaded power converters, LED driving systems can with high performances in terms

of efficacy, dynamic response, color control, cost effectiveness and compact in size can be realized.

Driver Topologies

There are two types of driver topologies for RGB LED. One is the non-isolated type including the basic topologies such as buck, buck-boost and boost converter [26, 27, 6, 28]. The other is the isolated type, including flyback, forward and Cuk converter and etc. Among the non-isolated topologies, buck converter is one of the most commonly used due to well developed topology and control, which provides it with fast dynamic response. Various control techniques, for example, V^2 control, hysteretic control, Constant-On-Time (COT) control and general current-mode control (peak and average mode) are available for buck topology [29, 30]. Buck-boost converter is not frequently used due to the inverted output. Boost type converter is another commonly used topology popular for driving high-voltage LED strings. However, the presence of the right hand plane zero complicates its control. For safety reasons, electrical isolation is sometimes required for LED drivers. The isolated topologies including flyback and forward converters, are suitable for this purpose [3, 31]. To avoid pulsating input current for buck converter and output current for boost converter, Cuk converter is developed for obtaining non-pulsating input, output current and hence reducing EMI problems, but its inverted output remains an important shortcomings [12].

Driving Techniques

HB LEDs are typically driven (or dimmed) by Amplitude Modulation (AM) and Pulse Width Modulation (PWM). It was found that LED driven by AM offers

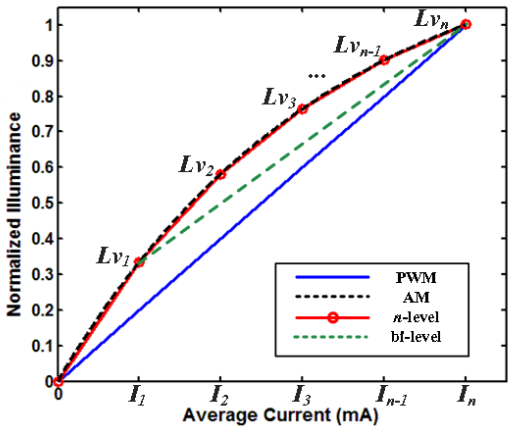

Figure 1-12: Illustration of a general *n*-section variable bi-level driving method.

the highest luminous efficacy, but dimming with AM is non-linear and it is difficult to achieve precise dimming. The other driving/dimming technique, PWM, offers linear dimming but poor luminous efficacy. Bi-Level current driving technique [32] and multi-level current driving technique [33] were proposed. The bi-level driving method is based on the superposition of a DC offset to a PWM current for improving the luminous efficacy from that with PWM current alone, as shown in Fig.1-12. The contribution of the current level Lv_n and Lv_1, having a lower and higher efficacy, is reduced and enhanced, respectively, thus increasing the overall luminous efficacy. However, the main drawback of the bi-level approach is that the minimum average LED current is limited to Lv_1, which limits the possible dimming range in practical applications. The generalized *n*-level current driving technique extends the bi-level driving technique but dividing the overall dimming range into multiple bi-level sections.It helps to maximize the efficacy and approaches the AM driving technique. Despite that this method offer good efficacy and color stability [12], the driver control and circuities are complicated and has not been implemented with simple and cost-effective methods. Another driving/dimming approach is the hybridization of PWM and AM [34], this method is difficult to implement and the dimming control is

complex. In addition, the requirement on converter's dynamic response is high as the system must respond with high precise to a change of DC current level over a wide range.

Driver Configurations

By inspection of Eqn. (1.10), it can be deduced that a small change of forward voltage will cause a larger change of forward current in LED. Besides, the effects of junction temperature change and ageing will lead to a change in forward voltage [6, 35]. Therefore, the illuminance of LED is preferred to be regulated by controlling the LED forward current flowing directly.

There are three types of driver configurations adopted for driving RGB LED. The conventional one, as illustrated in Fig. 1-13(a), use a DC/DC pre-regulator to regulate the common output voltage at a fixed value. Since LED of different color have different forward voltage drops under same forward current, a current balancing circuit is required for maintaining the same forward current among them. Although this method is cost effective, it introduces extra power loss in the current balancing circuit and is thus inefficient. To overcome the poor power efficiency, three converters can be cascaded in parallel, as shown in Fig. 1-13(b) [22, 26]. However, the size of this configuration is bulky, the circuit is complicated and more expensive. Another type of driver configuration is based on the color sequential driving technique, as shown in Fig. 1-13(c) [3, 6, 15, 36]. It employs the idea of time division where the driver's output is shared by LED of different colors in a time sequential manner. LEDs of different colors are switched in and out at sufficiently high frequency to avoid flickering. this configuration is cost-effective, but the utilization of each LED group is reduced to 1/3. Moreover, the control of the sequence driving signal

is complicated and the converter is required to possess dynamic response due to the constant switching between different LED groups.

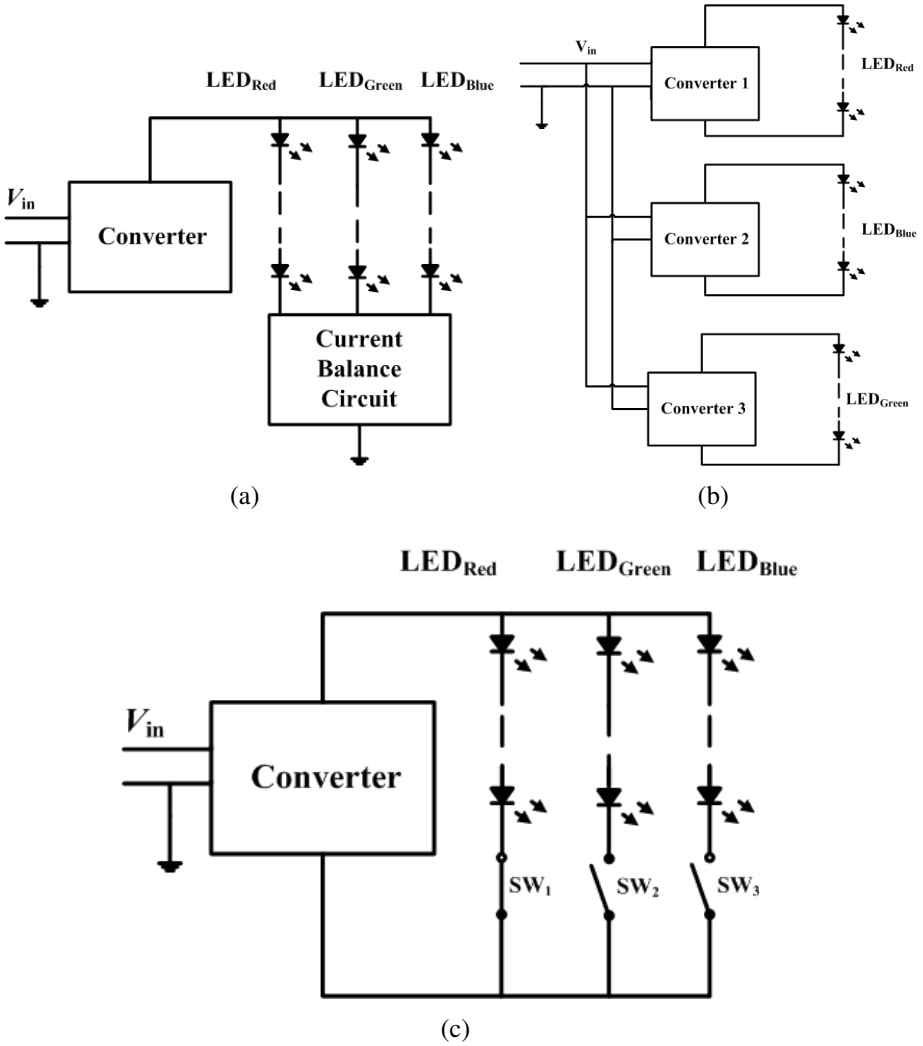

Figure 1-13: Cascaded topologies for RGB LED driving system.

2.4 Color Control of RGB LED

Since the luminous output of LED tend to change with their operating conditions, including current amplitude, ambient temperature (hence junction temperature) and ageing state, feedback control is typically required to maintain their luminous output

and compensate for the variations of these parameters. In particular, for RGB LED, since the overall CCT is a function of the luminous output of each primary-color LED, its control is heavily relying on the precise luminosity of each primary-color LED. A typical feedback control system for RGB LED is shown below.

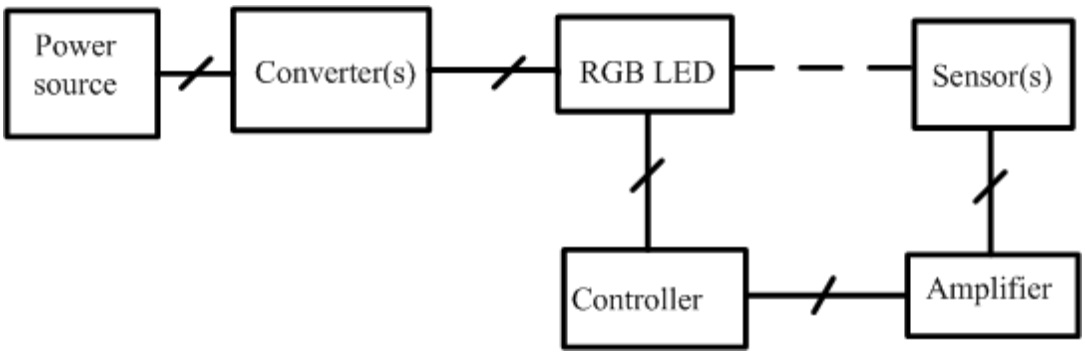

Figure 1-14: Block diagram of a general feedback control system for RGB LED driving system.

Fig. 1-14 is illustrating a general feedback control system for RGB LED including the driver stage. Generally, there are four components in the system: the power stage, LED sensor(s) and controller. The power stage can be formed by a AC or DC power source and a linear regulator or switching type converter(s).The controller can be analogue or digitally implemented, and preference is increasingly given to digital control due to its versatility. The sensor, can take different forms depending on the control objective. Fig. 1-15 shows a typical feedback control system based on PI compensator for regulating the lumionus output of each primary-color LED individually [26, 27].

Muthu *et. al* had proposed a optical sensing feedback control system based on the CIE1931 UCS tristimulus values [22, 26]. Besides, it is found that a higher precision dimming resolution is associated with a higher color precision. For Muthu's system, the range of overall CCT control from warm to 6500K is achieved with 0 to 80% of the change in dimming level. This implies that the 20% of the light output is

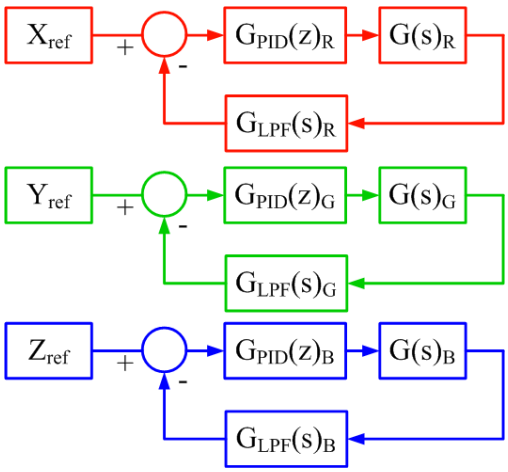

Figure 1-15: Block diagram of conventional RGB LED driver PI compensation.

reserved as headroom against the possible change of heat sink temperature. He found that when the heat sink temperature is increased by 50^{o}C, color variation exceeding the threshold will still occur despite the use of feedback control. This is due to the mismatch emitted spectrum and the CIE color matching functions. By this reason, a heat sink temperature feed forward scheme was incorporated into the optical feedback system in order to resolve the temperature dependency [37]. Apart from the optical sensing method and temperature feed forward method, another color control method was proposed by Qu *et. al* [27]. This method is based on the calibrated correlation between the forward vltage of LED and its junction temperature. Color variation is compensated through the detection of forward voltage. The method offers the advantage of not using optical sensors and free from the ageing problems of sensors. However, the ageing process of LED may cause a fault detection of the junction temperature change and hence incorrect color regulation. Hence, it requires regular calibration. In addition, the need for pre-calibration of many parameters (18 in total) is time consuming. Other than the aforementioned methods, a novel technique for regulating color instabilities was proposed. Sun [38] proposed a method that uses a self-aligned photo-power stabilization circuit for handling the luminos-

ity variation of RGB LED by estimating the optical power via the measurement of electrical power consumed by the red LED, therefore, it can be done without optical sensors. This method is able to maintain the luminosity variations to within 4%. However, information about the color variations was not discussed.

3 Objective

This thesis mainly focuses on two research problems related to RGB LED.

Firstly, driving solution for improving its efficacy compared to the conventional PWM method is found. From the literature review, it was found that the bi-level current or the *n*-level current driving technique are appropriate as the driving solution, but the complicated circuit implementation still imposes a significant challenge. A practical implementation of *n*-level driving technique, based on a digitally controlled color sequential dimming RGB LED driver system is presented in this thesis. It provides a practically viable implementation method for achieving a one-driver solution to drive RGB LED. Issue on color resolution and dimming approach are also discussed.

Secondly, a unified approach to controlling white color point of red/green/blue (RGB) LED existing in all ageing states. In contrast to conventional color control systems where the average driving currents of the primary-color LEDs can become saturated when the LEDs have undergone prolonged ageing, and causes the resulting white color point to go out of regulation, the proposed method avoids this problem by adjusting the color set-points when a pre-defined threshold current is reached by one or more of the primary-color LEDs. It is shown that the method can effectively maintain the white color point of the RGB LED at the desired value when the LEDs are subjected to an accelerated through repetitive current stress cycles.

4 Outline of the Thesis

Chapter 1 outlines some basics of LED and presents a literature review of LED driving and color control methods. Chapter 2 discusses a color sequential n-level one driver solution for RGB LED. Chapter 3 proposes a color control system for RGB LED with application to light sources suffering from prolonged ageing. Chapter 4 presents the conclusion and suggestions for future work.

Chapter 2

Sequential Variable Bi-Level Driving Approach Suitable for Use in High Color Precision LED Display Panels

1 Introduction

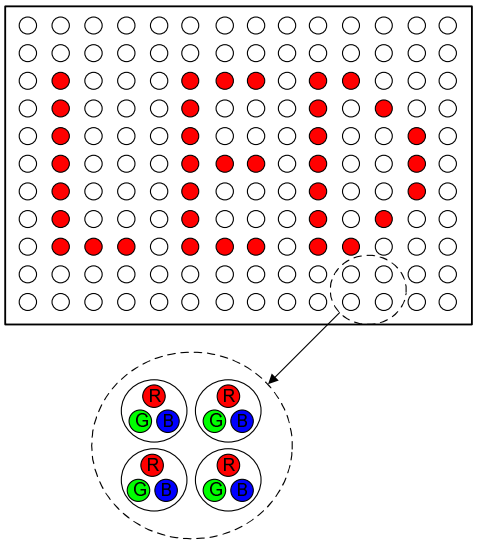

Figure 2-1: LED display panel containing matrix of RGB LEDs.

Currently large-area LED display panels are widely used as indoor and outdoor TVs for showing motion pictures and advertisements in public areas such as stadiums, shopping malls, concert halls, recreation and theme parks due to their versatility. A full-color LED display panel typically consists of a wide-area matrix of R(ed)-G(reen)-B(lue) LEDs arranged in two dimensions as shown in Fig. 2-1. In general, the image to be displayed is mapped onto the matrix of RGB LEDs, and the video signals representing the image are analyzed by video processing circuitry to determine the individual intensities of the primary-color light sources for every RGB LED on the panel. Each of the primary-color light sources is then driven according to the required intensity so that the desired color is obtained after mixing and the full image is displayed on the RGB LED matrix. Due to the fast electrical-to-light conversion of LEDs, the panel can be refreshed at a high frame rate for displaying motion pictures, thus forming an LED video screen. Compared to liquid crystal display (LCD) panels, no backlight is needed for LED display panels. Furthermore, unlike LCD panels that consist of glass component, LED display panels have a much better scalability and can be conveniently expanded in size by adding more LED modules and easily shaped for wall mounting, which make them well suited for a wide range of large-area display applications.

Pulse-width modulation (PWM) driving approach has been generally adopted for driving RGB LEDs since the individual intensities of the primary colors can be linearly controlled by adjusting the duty cycles of the PWM drive signals applied to them [39]–[40]. This also implies that the same color (after mixing) can be maintained under different dimming levels by keeping a constant duty cycle ratio between the three primary colors [37]–[26], which simplifies the driver design for RGB LEDs. However, it was reported in the some recent literatures that, since the luminous out-

put of LEDs tends to saturate at high current density, they generally suffer from a reduction in luminous efficacy when operated with a high peak current such as that encountered with PWM driving. This issue has been addressed by the bi-level driving approach proposed recently by the authors [41]–[32]; the main idea is to reduce the duration of time during which the LEDs are operated at high peak current. Based on the bi-level driving approach, the author of [33] further extended the idea and conceptualized the general *n*-level driving approach for further improving the luminous efficacy of LEDs.

The previous work reported in [33] mainly focuses on white LEDs and the improvement of their luminous efficacy by employing a multi-sectional piecewise-linear approximation to their luminous output curve under amplitude-modulation (AM) driving, which theoretically operates the LEDs with the highest luminous efficacy. The increased complexity of the driving approach generally necessitates the use of digital controller for programming the desired current levels and duty cycle and generating the corresponding drive signals to the LEDs. Therefore the total number of different current levels and duty cycle values that can be generated by the controller is dependent on the controller's bit resolution. In this thesis, it will be shown that, when the *n*-level driving approach is adopted for driving RGB LEDs, the availability of two degrees of freedom in luminosity control (current level and duty cycle) will lead to a significant improvement in color resolution compared to PWM driving implemented with a controller of the same bit resolution. Since LED display panels are constructed with RGB LEDs that are directly viewed by observers, the significant improvement in the color resolution is expected to enhance the color quality of the picture under display.

In this thesis, an example of digital implementation of the *n*-level driving ap-

proach is presented. For convenience, the driving approach is referred to as the *variable bi-level* driving approach in this thesis in order to emphasize its main feature of having non-static upper and lower current levels as compared to the static ones used in the conventional bi-level driving approach. The operating principles of the conventional bi-level and the variable bi-level driving approaches are briefly reviewed in Section 2. Design consideration and practical implementation of the driver system with digital micro-controller are discussed in Section 3, and experimental results are given in Section 4. Although the driving approach is implemented and verified for a single RGB pixel, the concept can be extended to a larger matrix such as an LED display panel. Section 5 presents the layout of a conceptual RGB driver for LED display panel based on the implementation method discussed in Section 3. Finally, conclusion is given in Section 5.

2 Variable Bi-Level Driving Approach

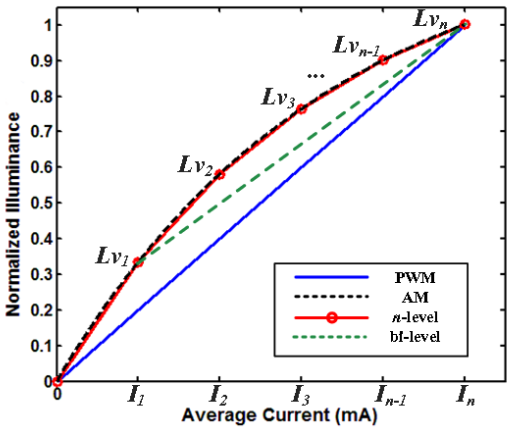

Figure 2-2: Illustration of a general n-section variable bi-level driving approach.

In comparison to the commonly used PWM driving approach, the bi-level driving approach operates by introducing a DC current offset into the PWM current such

that the modified current waveform pulsates between two non-zero current levels, denoted, for illustration, by Lv_1 and Lv_n joined by the green dashed line shown in Fig. 2-2. Due to the saturation effect of the luminous output of LEDs at high current, the luminous efficacy of LEDs generally decreases at high current. In comparison to the PWM driving approach, the presence of Lv_1 implies that the duty cycle applied to Lv_n can be decreased for attaining the same average current as the PWM case. As a result, the contribution of the current level Lv_n and Lv_1 having a lower and higher efficacy is reduced and enhanced, respectively, thus increasing the overall luminous efficacy. However, the main drawback of the bi-level driving approach is that the practical minimum average LED current is limited to Lv_1, which limits the possible dimming range in practical applications.

To overcome this limitation, by intuition, the LED can be further dimmed from Lv_1 to zero intensity by using a PWM current that pulsates between Lv_1 and 0. Therefore, the two-sectional driving approach, obtained by combining the first bi-level current (for dimming from Lv_n to Lv_1) and a second PWM current (for dimming from Lv_1 to 0), can be used to achieve the desired full-range dimming. Depending on the required average current, the driver circuit can be controlled to switch between the bi-level and the PWM mode, each behaving as a piecewise-linear approximation to the section acted upon by them. By taking the idea one step further, one realizes that adding more sections to the dimming approach also gives rise to a closer approximation to the luminous output curve of an AM-driven LED, which sets an upper limit to the maximum extractable luminous output from the LED, hence the overall luminous efficacy is improved.

Based on the prior description of the two-sectional approach, a general multi-sectional driving methodology, known as the variable bi-level driving approach, is

conceptualized and reported in [33]. It is designed to trace the luminous output curve of an AM-driven LED in a piecewise-linear manner by dividing it into multiple sections, as shown by the red curve in Fig. 2-2, where each section is bounded by a lower and upper current level(Note that the average current of each color is independent and can be controller by the user.). The intermediate current and luminosity values lying between the upper and lower current levels are obtained by duty cycle mixing of the two current levels. When the required average current and luminosity values exceed the range deliverable by one section, a new upper current level possessing a higher value will be generated to extend the operating range into the next higher section. In principle, the number of sections should be determined by the curvature of the AM luminous output curve and increased for a finer tracing resolution. However, the complexity of the driver circuit should increase with the number of sections used, hence a trade-off between the improvement in luminous efficacy and difficulty in implementation is usually required.

3 Design Consideration and Implementation of Driver System

3.1 Method for Generating Variable Bi-Level Current

Conventionally, three separate drivers are required to drive RGB LEDs since the three primary-color LEDs are characterized by different forward voltages. In order to minimize driver's size, a single-driver solution with current-mode control, and hence with dynamic bus voltage, is proposed in this section. The driver system is realized by using a single buck converter implemented by using LM3406 [42] as shown in Fig. 2-3(a), and the three primary-color LEDs are driven sequentially [36], [43] at

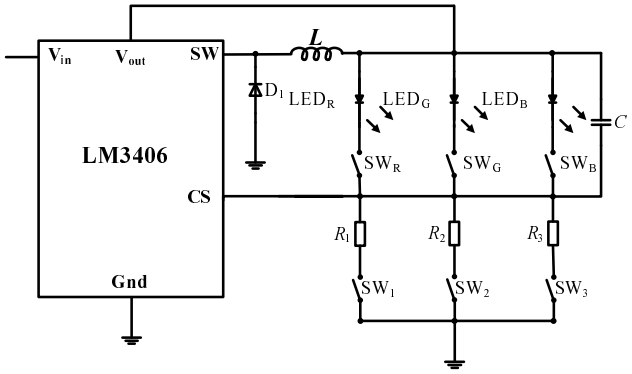

(a)

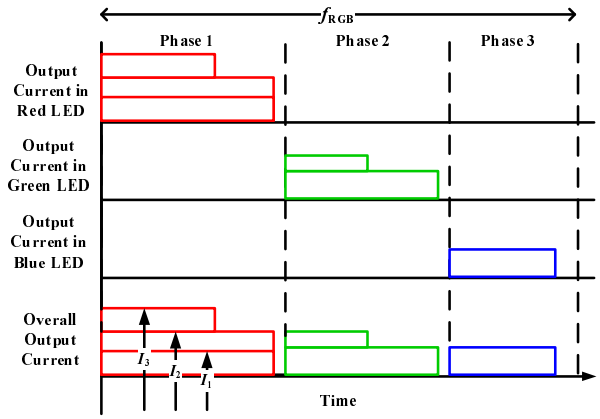

(b)

Figure 2-3: (a) Topology of the proposed RGB LED driver. (b) Illustration of the conceptual driving waveform for RGB LED.

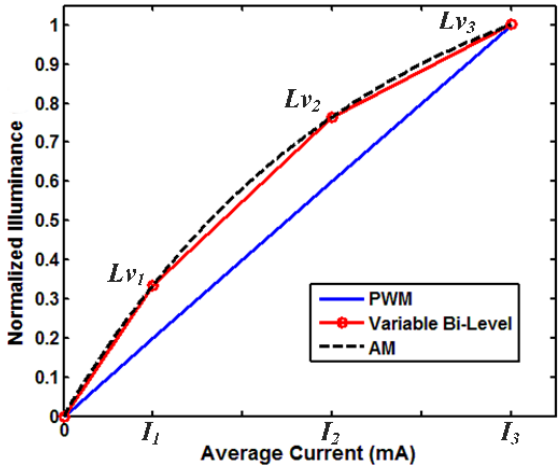

Figure 2-4: Illustration of a three-section variable bi-level driving approach.

the repetition frequency f_{RGB} as shown in Fig. 2-3(b). As a result, the maximum on-time for each primary-color LED is $T_{\mathrm{RGB}}/3$, where $T_{\mathrm{RGB}} = 1/f_{\mathrm{RGB}}$. To avoid the detection of flicker by human eyes, f_{RGB} is chosen to be 300 Hz hence the transition frequency between the three phases of the primary-color LEDs is 900 Hz. The luminous output curves of the three primary-color LEDs under AM driving were measured and three piecewise-linear sections are found to produce good approximations to these curves. Therefore, the driving waveform for the LEDs is characterized by one PWM section, *i.e.* $(0 \rightarrow I_1)$, and two bi-level sections, *i.e.* $(I_1 \rightarrow I_2)$ and $(I_2 \rightarrow I_3)$, as shown in Fig. 2-4. The buck converter is designed to operate in the current regulation mode for realizing these currents by selecting the current sense resistors according to the following equations (V_{ref} = 0.2 V). Note that hysteresis should be installed in order to avoid ambiguous between the adjacent level sections (e.g. $I_1 \rightarrow I_2$).

$$\begin{aligned} \frac{V_{\mathrm{ref}}}{I_1} &= R_1 \\ \frac{V_{\mathrm{ref}}}{I_2} &= R_1 // R_2 \\ \frac{V_{\mathrm{ref}}}{I_3} &= R_1 // R_2 // R_3 \end{aligned} \tag{2.1}$$

In the proposed driver, the selection of current level is realized by controlling the three MOSFET switches SW_1, SW_2, and SW_3 as shown in Fig. 2-3(a). The lowest section operates between 0 and I_1 realized by controlling the duty cycle applied to SW_1. When the required average LED current exceeds I_1, the next higher section is utilized, which operates between I_1 and I_2 realized by keeping SW_1 on at all time and controlling the duty cycle applied to SW_2. Similarly, when the required average

LED current exceeds I_2, the last section is utilized, which operates between I_2 and I_3 realized by keeping SW_2 on at all time and controlling the duty cycle applied to SW_3.

The sequential driving of the three primary-color LEDs is realized by controlling the three MOSFET switches SW_{R}, SW_{G}, and SW_{B} connected in series with the LEDs as shown in Fig. 2-3(a). The control signals to these switches are shifted by 120$^{\mathrm{o}}$ in phase or $T_{\mathrm{RGB}}/3$ in time with each other for generating non-overlapping gate drive signals for the different color phases. The sequential driving control signals for SW_{R}, SW_{G}, and SW_{B}, and the current selection control signals for SW_1, SW_2, and SW_3 for generating various colors and luminosity values are programmed into a single general-purpose micro-controller. Due to the turn-on and turn-off delay of the switches and the delay within the micro-controller with which the driving scheme is implemented, a minimum dead time t_d should be inserted between any two color phases, hence this limits the maximum average current of each primary-color LED $I_{i(\max)}$, where *i*=R,G,B, and the maximum converter's average output current $I_{o(\max)}$ to

$$\overline{I}_{i(\max)} = \left(\frac{V_{\mathrm{ref}}}{R_1//R_2//R_3}\right)\left(\frac{1}{3} - \frac{t_d}{T_{\mathrm{RGB}}}\right) \tag{2.2}$$

$$\overline{I}_{o(\max)} = 3\overline{I}_{i(\max)} \tag{2.3}$$

Since the source terminals of the floating switches SW_{R}, SW_{G}, and SW_{B} are kept constant at a low voltage V_{ref} = 0.2 V, the gate drive signals produced by the micro-controller are typically much higher than V_{ref} and ensure that these switches are turned on or off correctly without requiring floating gate drive circuits.

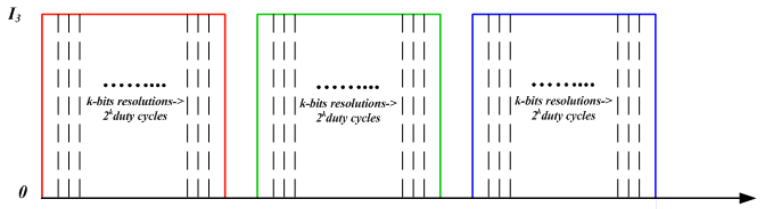

(a) PWM

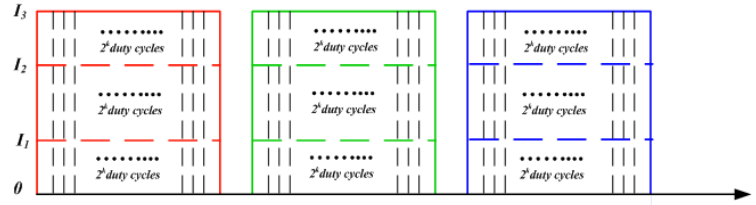

(b) Variable Bi-Level

Figure 2-5: Illustration of the color resolution property of a) PWM, and (b) variable bi-level driving.

3.2 Comparison of Color Resolution Between Variable Bi-Level and PWM Driving Approach

Given that a micro-controller can output gate drive signals at an *k*-bit resolution, the total number of discrete duty cycle values that can be generated by the micro-controller is 2^k.By referring to Fig. 2-5, this results in an intensity control of each primary-color LED to a resolution of $1/2^k$. Therefore, when driven by PWM, the total number of colors producible by mixing the three primary-color LEDs is given by $2^k \times 2^k \times 2^k = 2^{3k}$, equivalent to an overall system's color resolution of $3k$ bits.

With the variable bi-level driving approach, in general, *n* current levels are selected for realizing the intensity control of each primary-color LED and a resolution of $1/\left[n\left(2^k\right)\right]$ is achieved. The total number of colors producible by mixing the three primary-color LEDs is therefore given by $n\left(2^k\right) \times n\left(2^k\right) \times n\left(2^k\right) = n^3\left(2^{3k}\right)$, equivalent to an overall system's color resolution of $(3k + 3\log_2 n)$ bits. Hence, an effective improvement of $3\log_2 n$ bits in color resolution is achieved. However, since

the improvement in color resolution is proportional to $\log_2 n$, its effectiveness is diminishing with increasing n whereas the number of switches required for implementation increases linearly with n ($= 3 \times N_{\text{pixel}} \times n$).

Since three current levels ($n = 3$) are chosen in our implementation, and a micro-controller with an output resolution of 8 bits is used, it can be shown that the color resolution realizable by the proposed driver system has improved from 24 bits to $\approx$28.8 bits. Theoretically, in our implementation, the total number of colors producible with the variable bi-level driving approach is $\approx$453 millions compared to $\approx$16.8 millions obtained with the PWM driving approach. The improvement in color resolution is obtained with the same micro-controller, and hence no additional cost is required.

3.3 Dimming Approach

When dimming RGB LED, the intensity of each primary-color LED should be adjusted individually while keeping the intensity ratio between the three primary-color LEDs constant for a consistent color over dimming. When the RGB LED is driven by the PWM driving approach, this can be done easily by keeping a constant ratio between the duty cycle values used to operate the three primary-color LEDs. This is possible since, by referring to Fig. 2-4, dimming linearity with PWM ensures that the LED's luminous intensity is directly proportional to the PWM's duty cycle. However, when the three-sectional variable bi-level driving approach is adopted, the duty cycle required for attaining a given luminous intensity must be computed by the micro-controller from the known piecewise-linear parameters used to approximate the AM-driven luminous output curve, and the same is done for each of the three primary-color LEDs as follows.

Assume that the luminous output curves of the three primary-colors are approximated by three piecewise-linear sections described by the following equations, where *i*=R,G,B.

$$y = \begin{cases} m_{i,1} \cdot \overline{I}_i & 0 < y < Lv_1 \\ m_{i,2} \cdot \overline{I}_i + c_2 & Lv_1 < y < Lv_2 \\ m_{i,3} \cdot \overline{I}_i + c_3 & Lv_2 < y < Lv_3 \end{cases}$$

For a given required average luminous intensity y, the corresponding average LED current is given by

$$\overline{I}_i = \begin{cases} y/m_{i,1} & 0 < y < Lv_1 \\ (y - c_2)/m_{i,2} & Lv_1 < y < Lv_2 \\ (y - c_3)/m_{i,3} & Lv_2 < y < Lv_3 \end{cases}$$

Hence, letting $u = (1/3 - t_d/T_{\mathrm{RGB}})$, the required duty cycle value is given by

$$D = \begin{cases} \overline{I}_i/(uI_1) & 0 < y < Lv_1 \\ \left(\overline{I}_i/u - I_1\right)/(I_2 - I_1) & Lv_1 < y < Lv_2 \\ \left(\overline{I}_i/u - I_2\right)/(I_3 - I_2) & Lv_2 < y < Lv_3 \end{cases}$$

4 Experimental Results and Discussion

4.1 Hardware Implementation

$$L = \frac{V_{in} - V_o}{\Delta I_L} \times T_{on} \tag{2.4}$$

Fig. 2-6 shows the power stage of the proposed RGB LED driver. The converter's design is based on the application note of the constant current buck regulator

Table 2.1: Specifications of the proposed RGB LED driver implemented with variable bi-level driving approach.

Parameter	Symbol	Nominal Value
Converter's input voltage	V_{in}	12 V
Diode voltage	$V_{\text{o,R}}$	6.44 V
	$V_{\text{o,G}}$	8.58 V
	$V_{\text{o,B}}$	8.44 V
Current levels	I_1	506 mA
	I_2	756 mA
	I_3	1249 mA
Maximum average output current	$\overline{I}_{\text{o(max)}}$	1083 mA
Converter's switching frequency	f_{sw}	500 kHz
Sequential RGB repetition frequency	f_{RGB}	300 Hz
Dead time between two color phases	t_d	148 μs
Converter's output inductance	L	33 μH
Converter's output capacitance	C	470 nF
Current sense resistors	R_1	0.3 Ω
	R_2	0.7 Ω
	R_3	0.3 Ω

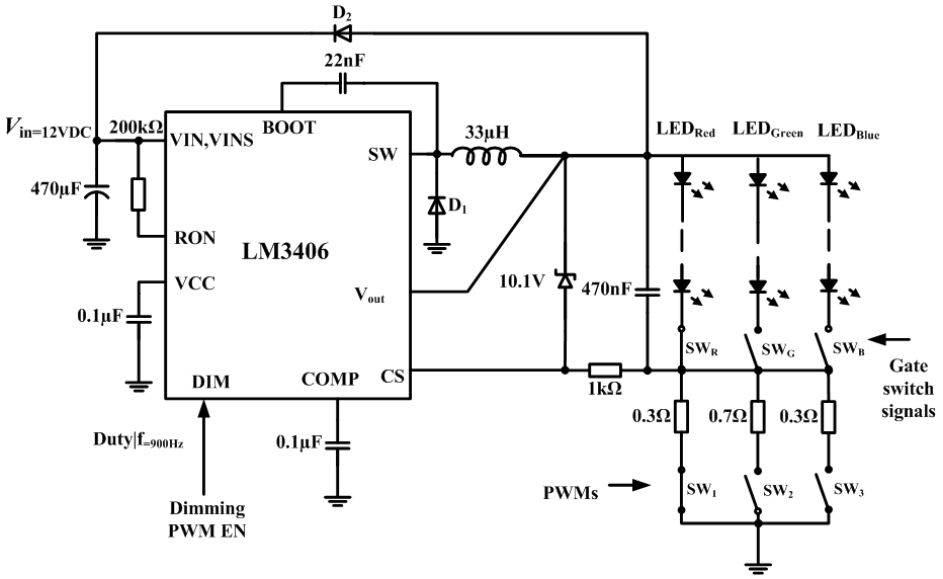

Figure 2-6: Schematic of power stage of high power RGB LED VBL driver.

controller IC, LM3406. The inductance value of the inductor is calculated by using Eqn.(2.4). The inductor's current ripple, ΔI_L , is set to be 15% of the maximum DC

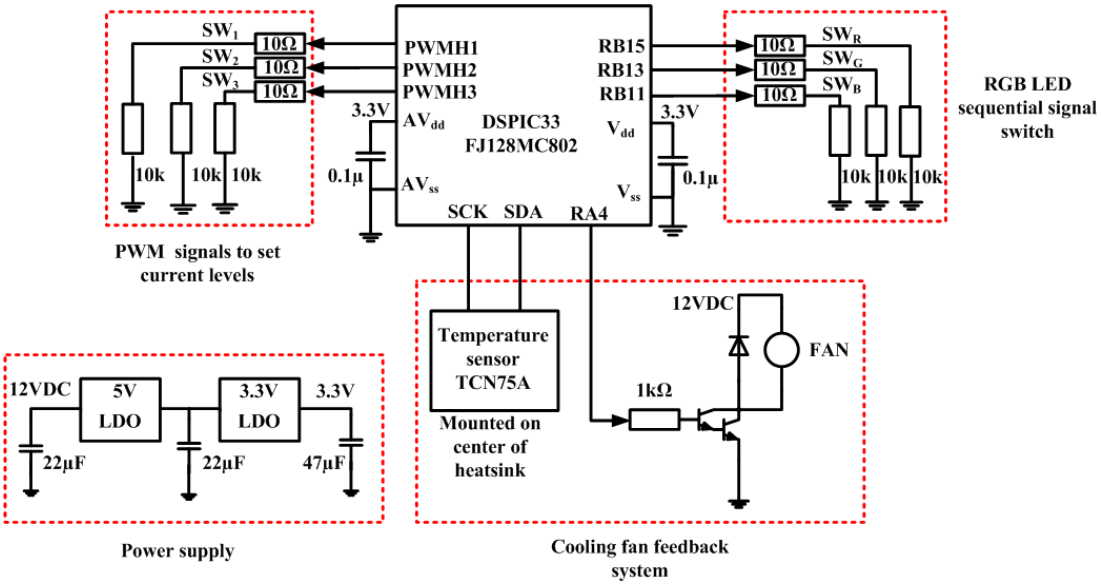

Figure 2-7: Schematic of the DSP controller of high power RGB LED driver.

Table 2.2: Parameters on the power stage design.

Parameter	R	G	B
L	31.92 μH	28.8 μH	28.08 μH
LED voltage (@0.5A)	4.971 V	7.057 V	6.805 V
LED voltage (@0.725A)	5.41 V	7.55 V	7.38 V
LED voltage (@1.25A)	6.447 V	8.587 V	8.44 V
$\mathrm{Duty_{LV1}}$@0.5 A	0.414	0.588	0.567
$\mathrm{Duty_{LV2}}$@0.725 A	0.451	0.629	0.615
$\mathrm{Duty_{LV3}}$@1.25 A	0.537	0.716	0.703

current or 187.5 mA . The inductance value is chosen based on the maximum value shown on Table 2.2 for compliance with the inductor current ripple requirement of all three primary-color LED groups. A zener diode and a resistor($1\mathrm{k}\,\Omega$) are use to limit the output voltage to a maximum value, e.g. all three switches ($\mathrm{SW_{1,2,3}}$) are turned off. A diode, $\mathrm{D_2}$ is used to protect the circuit from voltage surge originating from the inductor by clamping the maximum output voltage only to $\mathrm{V_{in}} + \mathrm{V_D}$. A $0.1\ \mu\mathrm{F}$ capacitor is connected to COMP for stabilizing the internal feedback loop. The dimming duty cycle signal is applied to the DIM pin in synchronization with the

switches ($\mathrm{SW}_{1,2,3}$).

The proposed RGB LED driver is implemented with the parameter values shown in Table 2.1. Each of the MOSFET switches SW_1, SW_3, and SW_3 has an on-resistance $R_{DS(on)}$ of 0.08 Ω and contributes to the total current sense resistor in each current path, hence it must be subtracted when calculating the current sense resistor values by equations (2.1). Hence, for example, the actual current sense resistor for the current path defining I_1 is $R_1' = R_1 + R_{DS(on)}$=0.38 Ω, and similarly for R_2'=0.78 Ω and R_3'=0.38 Ω. Both PWM and variable bi-level driving modes can be implemented by using the same converter. In the former case, all three switches SW_1, SW_2, and SW_3 are turned off during the PWM's off-time so that no current flows through the LED.

Fig. 2-7 shows the schematic of the DSP controller of the RGB LED driver. The dimming signal and sequential color switching signal are driven by the digital controller dspic33f128mc802. All gate signal pins have a $10\ \Omega$ connected in series in order to avoid switching glitch. Moreover, a pull down resistor ($10\ \mathrm{k}\Omega$) is connected to ground in order to ensure the switches can be fully turned off.

There is a temperature control system for regulating the heat sink's temperature. The cooling system is integrated with a DC fan and a temperature sensor. The temperature sensor is mounted under the center of the heat sink and the cooling fan is installed next to the heat sink. When the temperature rises more than $0.5\ ^{\mathrm{o}}\mathrm{C}$ from the target temperature, the DC fan will be turned for cooling down the heat sink, and it will be turned off when the temperature falls below its set value by $0.5\ ^{\mathrm{o}}\mathrm{C}$.

Samples of captured PWM and variable bi-level current waveforms are shown in Fig. 2-11 and Fig. 2-12, respectively. The fast transitions of the current waveforms between different current levels indicate a very good converter's dynamic response.

4.2 Power Consumption of Buck Regulator Employing Sequential Variable Bi-level Driving

The energy efficiency based on the input and output power: The input electrical power can be calculated from the experimental rms input current :

$$\begin{aligned}
\begin{bmatrix} P_{in(R1)} & P_{in(R2)} & P_{in(R3)} \\ P_{in(G1)} & P_{in(G2)} & P_{in(G3)} \\ P_{in(B1)} & P_{in(B2)} & P_{in(B3)} \end{bmatrix} &= V_{in} \times \begin{bmatrix} I_{in(Rlv1)} & I_{in(Rlv2)} & I_{in(Rlv3)} \\ I_{in(Glv1)} & I_{in(Glv2)} & I_{in(Glv3)} \\ I_{in(Blv1)} & I_{in(Blv2)} & I_{in(Blv3)} \end{bmatrix} \\
&= 12\,V \times \begin{bmatrix} 0.288 & 0.425 & 0.830 \\ 0.361 & 0.540 & 1.017 \\ 0.350 & 0.525 & 0.970 \end{bmatrix} A \\
&= \begin{bmatrix} 3.456 & 5.10 & 9.960 \\ 4.332 & 6.48 & 12.204 \\ 4.200 & 6.30 & 11.640 \end{bmatrix} W
\end{aligned} \tag{2.5}$$

The averaged input electrical power, when three primary-color LEDs are at the same current level, can be obtained by the averaging the values belonging to the same colum in Eqn. (2.5):

$$\overline{\mathbf{P}}_{\mathbf{in}} = \begin{bmatrix} 3.9960 \\ 5.9600 \\ 11.2680 \end{bmatrix} W \tag{2.6}$$

Thus the averaged energy efficiency when the buck regulator operates at different

output current levels are:

$$\overline{\eta}_{\mathbf{P_o},\mathbf{P_{in}}} = \begin{bmatrix} 79.479\,\% \\ 82.584\,\% \\ 86.732\,\% \end{bmatrix} \tag{2.7}$$

4.3 Software Implementation

Table 2.3: Programming Tools.

Tools	Name
DSP	DSPIC33FJ128MC802
Computer Language	C
Software (IDE)	Microchip MPLab X
Computing speed	40 MIPS

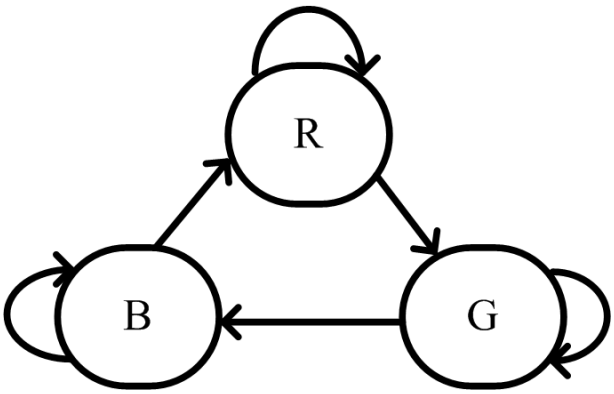

Figure 2-8: State machine of the RGB driving system, each internal node is shown in Fig. 2-9

Basically, the firmware design is developed by using Microchip X lab IDE environment. The computer language is embedded C with a DSP micro-controller (40 MIPS). The state machine of the RGB LED driving system is shown in Fig. 2-8. The sequential RGB color switching signal rotates with time as driven by a state machine. In the state machine, there are three nodes representing three color

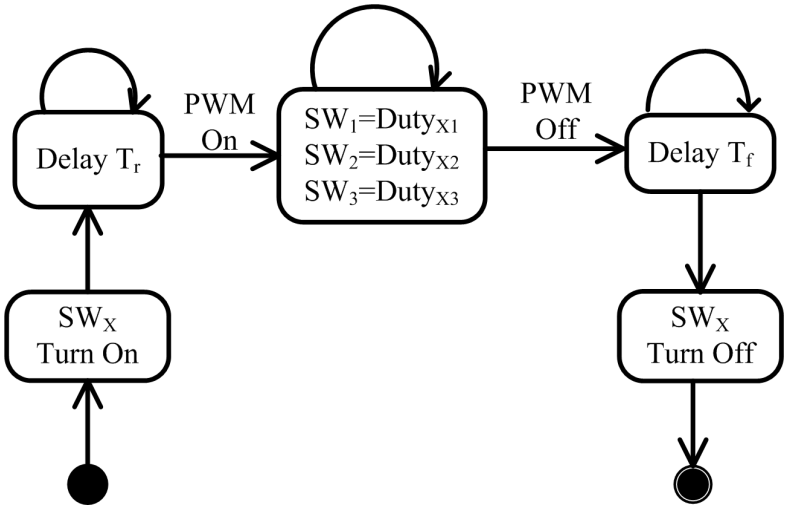

Figure 2-9: State machine per RGB node, where X=R or G or B

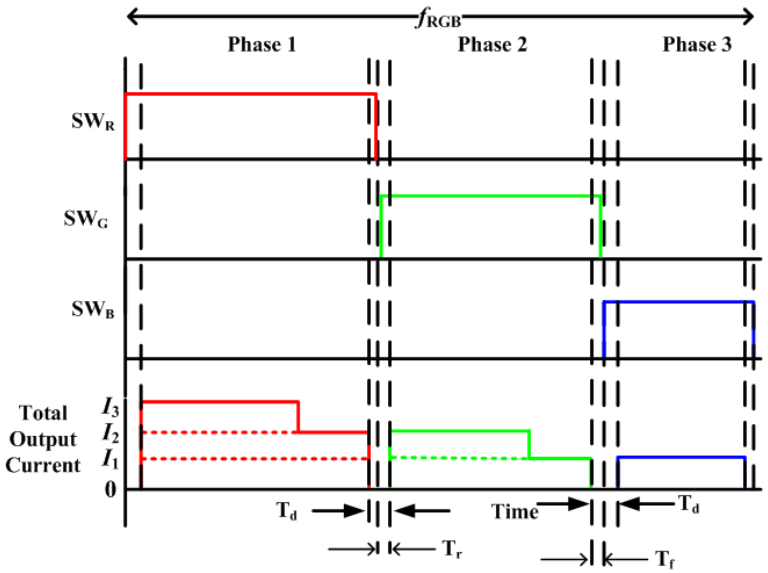

Figure 2-10: Delays (T_r, T_f) should be applied before and after current passes though an LEDs .

states. Each state node is identical as shown in Fig. 2-9. Every node is sequentially activated. Every primary-color LED starts to turn on with the activation of its respective switch, SW_X, where X=[R,G, B]. A certain rise time delay is introduced to avoid glitch from the DC-DC converter ,and also to ensure that the current path to the inductor is complete. $SW_{1,2,3}$ are then activated with PWM signals to deliver

the required VBL current. This node's state ends with a certain fall time delay to avoid a sudden cut off of the inductor current path before turning the SW_X off. This node state ends with switching to next color node state. Fig. 2-10 shows the time waveforms of the LED current.

4.4 Results

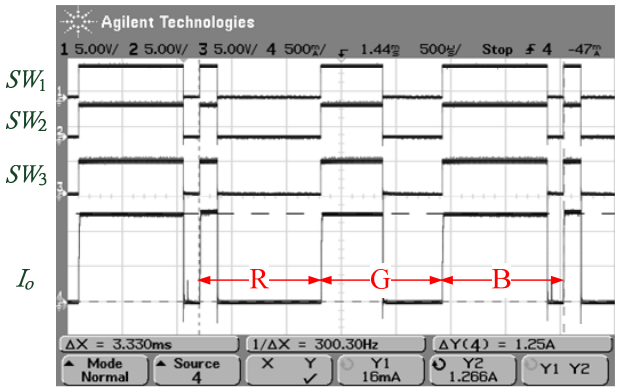

Figure 2-11: Sample of captured PWM current waveform.

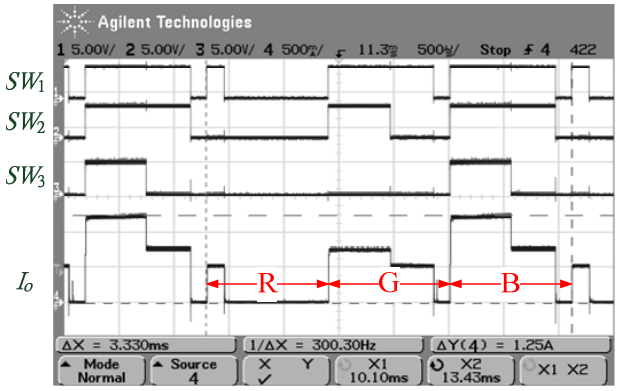

Figure 2-12: Sample of captured variable bi-level current waveform.

A comparison of the normalized illuminance of each primary-color LED under PWM and variable bi-level driving approach is shown in Fig. 2-13. In general, the variable bi-level driving approach produces a higher illuminance under all average

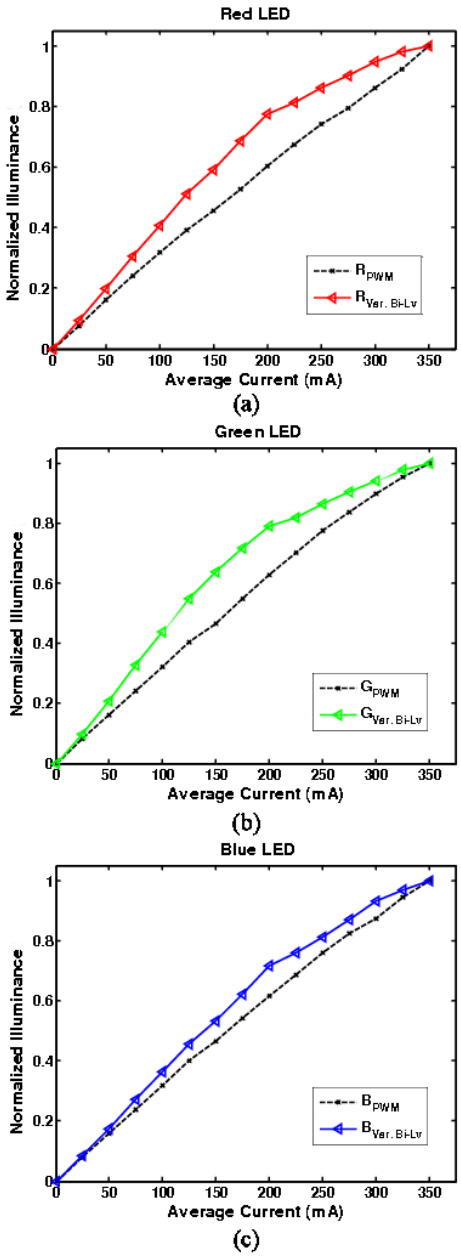

Figure 2-13: Comparison of measured illuminance of Lamina NT-43F0-0424 RGB LED under variable bi-level and PWM driving.

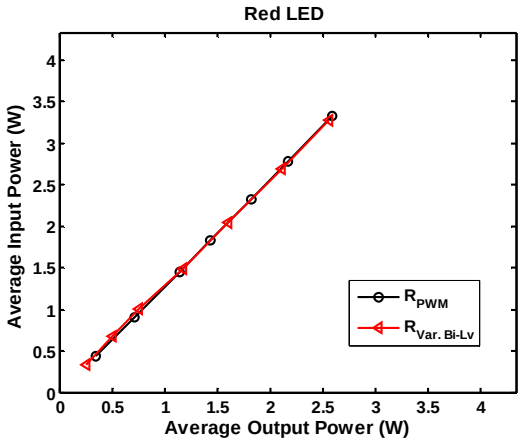

(a)

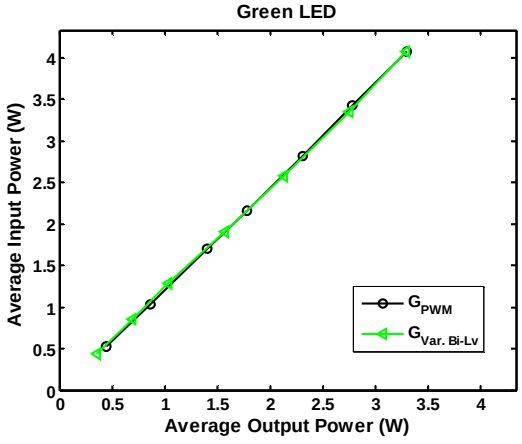

(b)

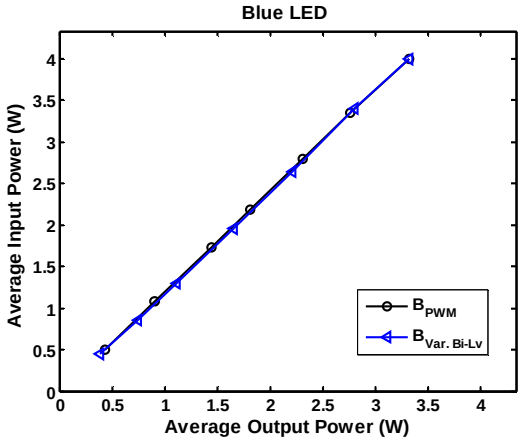

(c)

Figure 2-14: Comparison of measured driver's input and output power under variable bi-level and PWM driving.

current conditions. For the PWM case, the linear relationship between the illuminance and average current is evident from the plots having a constant slope. On the other hand, for the variable bi-level case, such a linear relationship is characterized by different slopes for different piecewise-linear sections of the illuminance curve. A maximum illuminance gain due to variable bi-level driving is found in the mid-range average current with 30.2 %, 37.0 %, and 16.4 % obtained for the red, green, and blue LED, respectively. The average illuminance gain over the full-range average current is 20.5 %, 20.8 %, and 9.7 % for the red, green, and blue LED, respectively. It should be emphasized that when video images are displayed on an LED display panel, the intensities of the RGB LEDs are generally varying with time hence the time-averaged currents and intensities are expected to lie in the mid-range region where the illuminance gain obtained is the most significant.

Fig. 2-14 shows that despite the added circuit's complexity with the implementation of the variable bi-level driving scheme, there is virtually no difference between the driver's efficiency under PWM and variable bi-level driving. This verifies that the overall electrical-to-light conversion efficiency will be improved by adopting the variable bi-level driving approach.

Finally, the effectiveness of the dimming approach proposed in Section 3.3 is verified by measuring the CIE 1976 color coordinates (u', v') of the RGB LED sample under different dimming levels. The color used for the test corresponds to the color obtained when each primary-color LED is driven with the rated current of 350 mA, which defines the rated intensity represented by the dimming level 10. The full dimming range is divided equally into ten intervals and the corresponding current levels and duty cycles required for each dimming level are calculated by the micro-controller using the formula given in Section 3.3. It can be seen from the

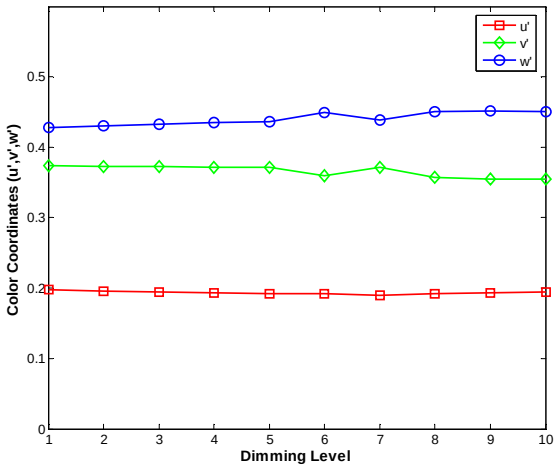

Figure 2-15: Measured color coordinates of Lamina NT-43F0-0424 RGB LED at different dimming levels under variable bi-level driving.

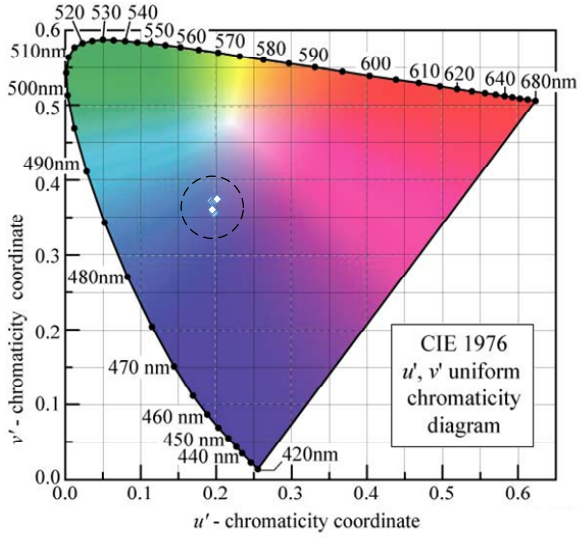

Figure 2-16: Measured color coordinates of Lamina NT-43F0-0424 RGB LED at different dimming levels plotted on the CIE 1976 chromaticity diagram.

measured color coordinates (u', v') shown in Fig. 2-15 that a stable color is maintained by the dimming approach over the full dimming range without closed-loop color stabilization. The plot of the measured color coordinates at different dimming levels on the CIE 1976 chromaticity diagram is shown in Fig. 2-16 by the area enclosed by the dashed line, which provides an alternative view to the stability of the test color point over the full dimming range. For LED display panels, installations

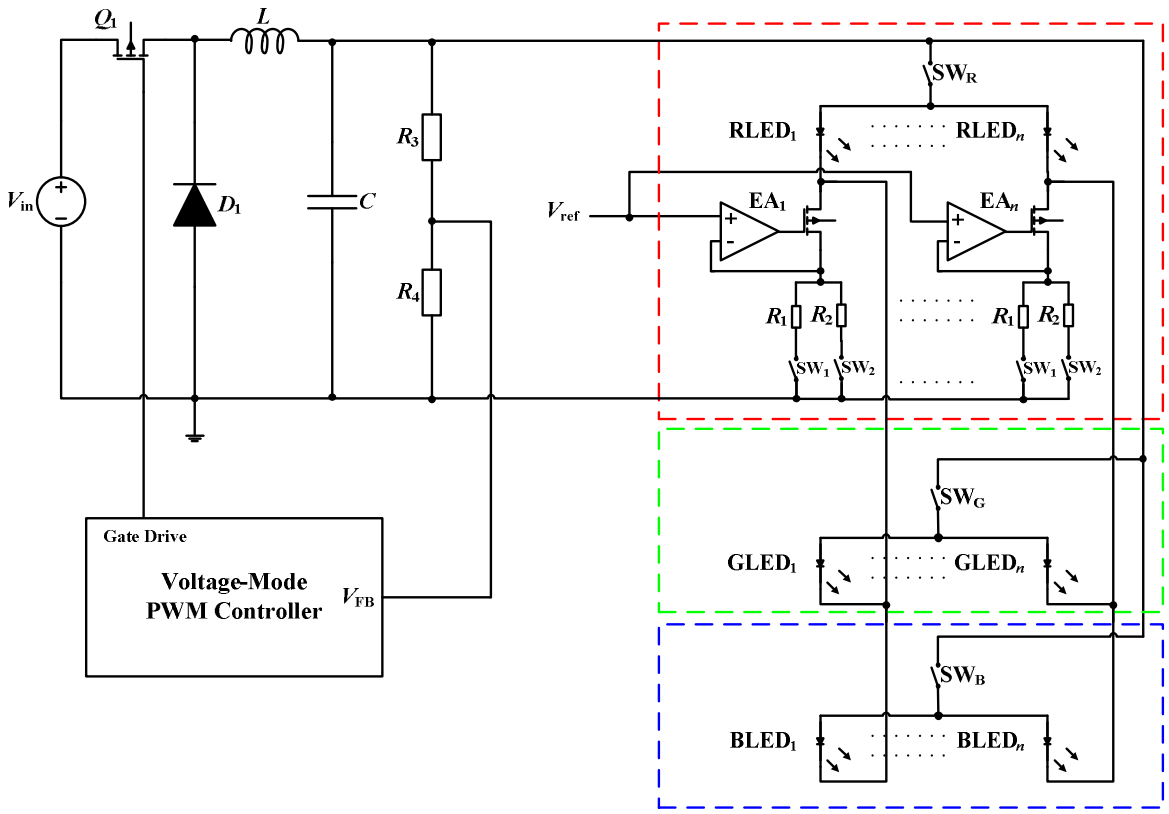

Figure 2-17: A buck-type RGB LED driver implemented with sequential variable bi-level approach for driving LED display panel.

of color sensors and feedback control circuitry for color stabilization are not feasible since a large number of RGB LEDs must be monitored and the images to be displayed are typically non-static. In this case, the color stability demonstrated by the proposed dimming approach ensures that a given color is displayed accurately at different dimming levels as required by the image being displayed.

5 RGB LED Driver for LED Display Panel

The merits of the variable bi-level driving approach were discussed in the previous sections and verified on a single RGB LED pixel. In this section, an attempt is made to scale up the RGB LED driver demonstrated in Section 3 to one suitable

for use in a larger matrix such as an LED display panel. The schematic of a sample design is shown in Fig. 2-17, which is based on the design proposed in [28]–[35] for driving multi-string LED arrays and was later adapted for driving LED display panels in [44]. Since every pixel needs to be driven individually, all RGB LEDs on the panel should be arranged in parallel, and a buck converter is chosen since the required output voltage is typically lower than the available input voltage from the prior AC-DC conversion stage. Specifically, the buck converter's output voltage should be designed to be not much higher than the highest per-LED forward voltage among the three primary-color LEDs in order to minimize the voltage drop across, and hence the power loss in, the linear regulators. In [28]–[35], this is achieved by threshold detection of MOSFET's drain voltage and dynamic bus voltage regulation.

The proposed architecture in [44] is further adapted here to incorporate the variable bi-level driving approach. The RGB pixels on the panel are generally divided into three primary-color groups. Each LED string within a primary-color group consists of one LED, and its forward current is regulated by linear current regulator formed by an error amplifier, a MOSFET, and current sense resistors. Since the forward currents through the LEDs are regulated individually by linear regulators, the buck converter is designed to operate in the voltage-control mode. For illustration, a two-sectional variable bi-level driving scheme is adopted by using two current sense resistors R_1 and R_2, thus giving rise to a PWM section between zero and $I_1 = V_{\rm ref}/R_1$ and a bi-level section between I_1 and $I_2 = V_{\rm ref}/\left(R_1||R_2\right)$. The average forward current for each LED is controlled by adjusting the duty cycle applied to SW_1 and SW_2. They are computed based on the time-varying video signals of the image under display. Finally, the three primary-color groups are driven sequentially in time by controlling the three non-overlapping switches $SW_{\rm R}$, $SW_{\rm G}$, and $SW_{\rm B}$ as

discussed in Section 3. Since the three primary-color groups are turned on sequentially, only one error amplifier per RGB pixel, for example EA_1, is required.

6 Summary

In this chapter, the recently proposed general *n*-level driving approach was revisited in the context of LED display panel with a more detailed study on its impacts on the luminous efficacy of RGB LED and the color resolution of display. It was shown experimentally that, compared to PWM driving, the luminous efficacy of the tested RGB LED has improved significantly with the use of two drive parameters, high/low PWM current levels and duty cycle, for piecewise-linear approximation to the DC luminous characteristic of LED. It was also shown by theoretical analysis that, when the driving approach is implemented with digital micro-controller, the system's color resolution generally improves by $3\log_2 n$ bits compared to PWM driving using the same micro-controller. The first practical implementation of a digitally controlled RGB LED driver employing the *n*-level driving approach was proposed and verified experimentally on a single RGB pixel. A further extension of the driver for driving LED arrays in LED display panel was also discussed. The proposed driver will be constructed and verified in the future. Due to the similarity in driving requirements, the extension of the driving approach to back-lit RGB backlight for LCD panels that employ *local dimming* technology [15]–[45] will also be considered.

Chapter 3

Color Control System for RGB LED with Application to Light Sources Suffering from Prolonged Ageing

1 Introduction

High-brightness LEDs have been increasingly used for applications that require high luminosity and color accuracy, such as in the backlight system for liquid crystal display (LCD) monitors and LED projectors [39]–[14]. These applications typically employ phosphor-coated white LEDs as the light source, and the drawback of using them is that the color temperature of the white light is pre-determined by the chemical composition of the phosphor used and not directly controllable by external means. In addition, the color temperature of phosphor-coated white LEDs can vary significantly during their service lifetime mainly due to the ageing of phosphor. This will lead to a degradation of color quality as a function of the service lifetime of LED light source in these applications.

For LED-based backlight system in smart phones such as iPhone, the problems of ageing and yellowing of backlight are known to cause discomfort to the users [19, 23]. For image display with multi-projector system, the projected image is strictly required to be seamless on the projected edge of each projector. Image distortion is not permitted and the alignment should be sufficiently well-balanced [46]–[47]. Besides, the users of multi-projector system also face the problem of color drift or non-uniformity between the different parts of the same image as the LED light sources of these projectors become aged [46]–[48]. The reason is that, in a multi-projector system, the brightness of the LED light sources of different projectors can decay at different rates, which renders the image under display to be non-uniformly shown in both luminosity and chromaticity [49, 50]. As a result, the image alignment between the projectors can be adversely affected. Recently, the DLP portable projectors produced by Texas Instruments have become available in the market [51], [52]–[16]. The size of their body should be compact and hence their inner structure should occupy a volume that is as small as possible. For these reasons, the flexibility in the design of circuitry is limited. Therefore, a color-sequential driver circuit is adopted as the driver solution, and since this type of driver typically imposes a high peak current on the LED light source, the design is expected to suffer from an accelerated ageing of the LED light source [20].

To cope with these limitations of phosphor-coated white LEDs, for color sensitive applications, an alternative method to produce white light that offers a better color control flexibility is obtained by mixing the light output of red, green, and blue (RGB) LED [22]. Since these primary-color LEDs are individually controllable through their driver circuits, the color temperature of the white light produced by this method is also tunable to give different viewing moods or sensations to the users. In

general, two different approaches have been proposed for controlling the color point of RGB LED.

In the first approach, no optical sensor is used in the feedback control. The forward voltages of the primary-color LEDs are measured in real-time and their junction temperatures and luminance are predicted from pre-calibrated curves [27]. In [38], the electrical power consumption of the primary-color LEDs are measured and used to predict their luminance. These methods, which are based on the measurement of electrical parameters, may lose their accuracy when the LEDs are aged and their electrical parameters have changed considerably from their initial values used in calibration. Fig. 3-1 shows the variations of the forward voltages of red, green, and blue LED (of Lamina NT-43F0-0424 RGB LED module) as a function of the ageing time in an accelerated lifetime test. Recently, a luminous control method based on thermal estimation has been proposed [53]. The method is based on a pre-calibrated estimator that provides the luminous flux of LED from the measured case and ambient temperatures. However, the ageing of the LED light sources may cause their luminous characteristics to deviate significantly from the ones used in the calibration of estimator. Moreover, the thermal estimator's model required for a RGB system will be significantly more complex than the one reported using white LEDs only.

In the second approach, optical sensors are used to detect the luminance of the primary-color LEDs and regulate them against some pre-defined references through PID controllers [26]. When their luminance deviate from the reference values, the changes are detected by optical sensors and the controllers will restore their luminance to the desired values in real-time. Since the luminance of LED typically decreases with ageing due to phosphor's deterioration, this implies that the average driving currents of the primary-color LEDs are bound to increase with ageing in or-

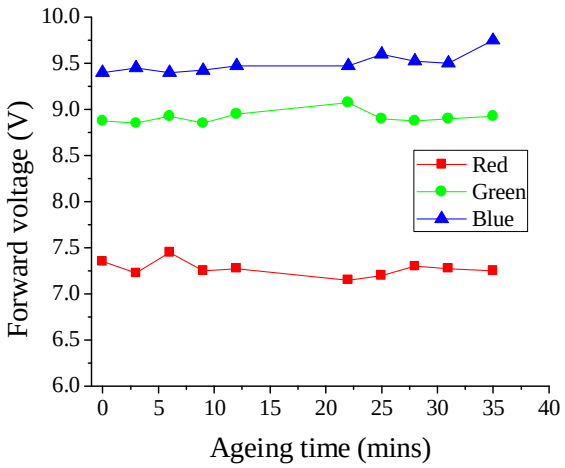

Figure 3-1: Variations of forward voltages of red, green, and blue LED (of Lamina NT-43F0-0424 RGB LED module) as a function of ageing time in an accelerated lifetime test.

der to keep the total luminance constant. This leads to the negative consequences of increased junction temperature and the risk of causing the average driving current to saturate at the upper limit. When the average driving current of one or more of the primary-color LEDs becomes saturated, *i.e.* reaches its upper limit, the feedback system will become open loop and it can no longer regulate the luminance of the primary-color LEDs, and the color point of the total luminance will deviate from the desired value as the LEDs age further.

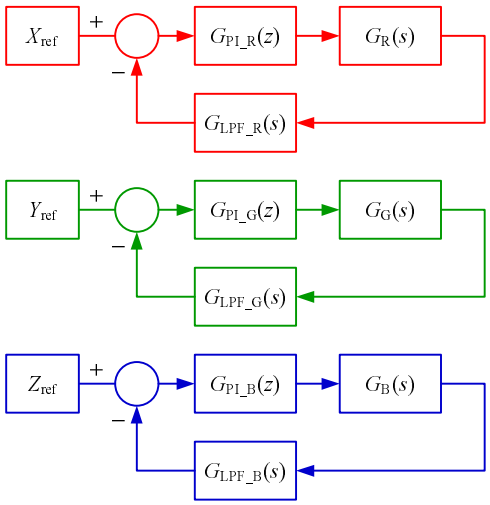

Figure 3-2: Block diagram of conventional RGB LED driver with color-sensing feedback control.

In this thesis, an optical-sensor-based RGB LED driver system that employs a new algorithm for preventing the saturation of driving current is proposed. A threshold current is imposed below which the system operates with normal PID control that regulates the luminance of the primary-color LEDs against some constant references, as shown in Fig. 3-2, and the total luminance and color point are kept constant. When the average driving current of one of the primary-color LEDs has reached the threshold current, its reference is dynamically adjusted in order to keep the average driving current fixed at the threshold value and to prevent it from increasing further. The references of the remaining two primary-color LEDs are modified accordingly in order to the keep the color point of the total luminance constant at the desired value. This method ensures that the color generated by the RGB LED remains constant throughout its service lifetime, and it is not driven by excessive current that will further accelerates its ageing.

The thesis is organized into five sections. Section 1 gives an overview of existing color control methods for RGB LEDs. Section 2 describes the concept of the proposed color control method taking into consideration the effect of ageing of RGB LED. Section 3 gives the implementation details of the proposed control system, and its validity is experimentally verified in Section 4. Finally, conclusions are given in Section 5.

2 Formulation of Control Algorithm

In the proposed RGB driver system, the primary-color LEDs are assumed to be driven by PWM current, whose peak value I_{peak} is kept constant and the average driving currents of the primary-color LEDs are individually controlled by varying their duty cycle. One driver is employed to operate the primary-color LEDs sequen-

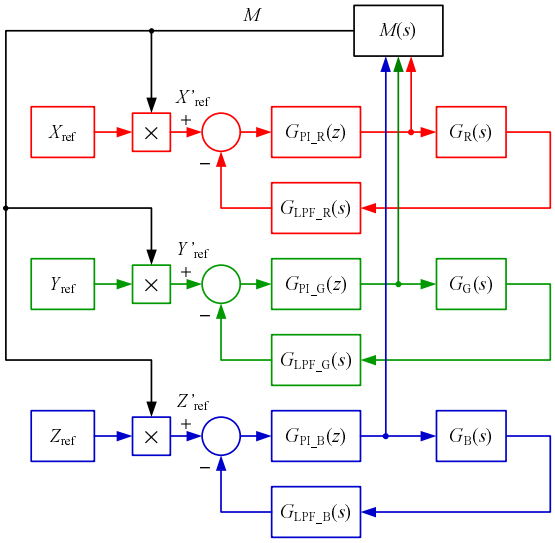

Figure 3-3: Block diagram of the proposed color control system including dynamic change of references.

tially by time division [54]. The luminance of each primary-color LED is sensed by the optical sensor that is sensitive to its emitted wavelength. The analogue luminance signal is then digitized and fed into a micro-controller unit (MCU) that computes the PWM duty cycle required to regulate the luminance of the primary-color LED at the desired value. Since there are areas of overlapping in the spectrum produced by the primary-color LEDs as well as in the detection windows of the optical sensors, only one primary-color LED and optical sensor pair is active at one time, therefore each primary-color LED and its associated optical sensor are turned on and off in synchronization with each other.

A threshold current I_{thres} is set as the boundary value that distinguishes the two operating modes (Mode I and II) of the system. Below the threshold current, *i.e.* Mode I, the average driving currents of the primary-color LEDs are adjusted by PID controllers in order to deliver the desired luminance according to the pre-defined references, hence the average driving currents generally increase as the LEDs age. Assuming that the luminance of the primary-color LEDs are perfectly tracked at their

references, the color point (x, y, z) of the total luminance is given by Eqn. (3.1), where $X_{\rm ref}, Y_{\rm ref}$, and $Z_{\rm ref}$ are the reference tristimulus values against which the luminance of the primary-color LEDs are regulated.

$$\begin{aligned} x &= \frac{X_{\rm ref}}{X_{\rm ref} + Y_{\rm ref} + Z_{\rm ref}} \\ y &= \frac{Y_{\rm ref}}{X_{\rm ref} + Y_{\rm ref} + Z_{\rm ref}} \\ z &= 1 - x - y \end{aligned} \tag{3.1}$$

When the threshold current is exceeded, the system enters into the second operating mode (Mode II), which gives rise to two possible cases: (1) When the average driving current of *one* of the primary-color LEDs has exceeded the threshold current, the condition is detected by the MCU and its reference is decreased in order to restore the average driving current to the threshold value; (2) When the average driving currents of *two* or *more* primary-color LEDs have exceeded the threshold current, the reference of the one that exhibits the largest decay in luminance (over ageing), and whose average driving current has exceeded the threshold current by the largest percentage, should be decreased in order to restore its average driving current to the threshold value, while the references of the remaining two primary-color LEDs are adjusted accordingly in order to keep the color point constant at the desired value.

The control method for Mode II's operation is formulated as follows. Since the luminance of PWM-driven LED is proportional to its duty cycle, when, after a sufficient ageing, the average driving current of one of the primary-color LEDs, for example, X, has exceeded the threshold current, *i.e.* $I_{\rm ave} > I_{\rm thres}$, the corresponding duty cycle D_X (equal to $I_{\rm ave}/I_{\rm peak}$) is detected by the MCU and compared to the critical duty cycle $D_{\rm cri}$ (equal to $I_{\rm thres}/I_{\rm peak}$). In order to restore its average driving current to $I_{\rm thres}$, a new reference $X'_{\rm ref}$ is calculated, and the references for $Y'_{\rm ref}$ and

Z'_{ref} are adjusted accordingly.

$$\begin{aligned} X'_{\text{ref}} &= \left(\frac{D_{\text{cri}}}{D_X}\right) X_{\text{ref}} \\ Y'_{\text{ref}} &= \left(\frac{X'_{\text{ref}}}{X_{\text{ref}}}\right) Y_{\text{ref}} = \left(\frac{D_{\text{cri}}}{D_X}\right) Y_{\text{ref}} \\ Z'_{\text{ref}} &= \left(\frac{X'_{\text{ref}}}{X_{\text{ref}}}\right) Z_{\text{ref}} = \left(\frac{D_{\text{cri}}}{D_X}\right) Z_{\text{ref}} \end{aligned} \tag{3.2}$$

This formulation ensures that the color point of the total luminance is kept constant, as shown by the calculations in Eqn. (3.3). Since $D_X > D_{\text{cri}}$, following the adjustment of the references, the total luminance will be reduced by a factor of $(1 - D_{\text{cri}}/D_X)$. In practice, since the ageing of LED is a very slow process, these adjustments are not expected to cause an abrupt fall in luminosity and visual discomfort to users.

$$\begin{aligned} x &= \frac{X'_{\text{ref}}}{X'_{\text{ref}} + Y'_{\text{ref}} + Z'_{\text{ref}}} \\ &= \frac{\left(\frac{D_{\text{cri}}}{D_X}\right) X_{\text{ref}}}{\left(\frac{D_{\text{cri}}}{D_X}\right) X_{\text{ref}} + \left(\frac{D_{\text{cri}}}{D_X}\right) Y_{\text{ref}} + \left(\frac{D_{\text{cri}}}{D_X}\right) Z_{\text{ref}}} \\ &= \frac{X_{\text{ref}}}{X_{\text{ref}} + Y_{\text{ref}} + Z_{\text{ref}}} \\ y &= \frac{Y'_{\text{ref}}}{X'_{\text{ref}} + Y'_{\text{ref}} + Z'_{\text{ref}}} \\ &= \frac{\left(\frac{D_{\text{cri}}}{D_X}\right) Y_{\text{ref}}}{\left(\frac{D_{\text{cri}}}{D_X}\right) X_{\text{ref}} + \left(\frac{D_{\text{cri}}}{D_X}\right) Y_{\text{ref}} + \left(\frac{D_{\text{cri}}}{D_X}\right) Z_{\text{ref}}} \\ &= \frac{Y_{\text{ref}}}{X_{\text{ref}} + Y_{\text{ref}} + Z_{\text{ref}}} \\ z &= 1 - x - y \end{aligned} \tag{3.3}$$

By extending the formulation further, when the average driving currents of two or more primary-color LEDs have exceeded the threshold current, the one that produces

the largest average driving current is selected by a routine M (see Fig. 3-4(b)) and adopted as the basis for adjusting the references of the remaining two primary-color LEDs. This can be mathematically expressed by Eqns. (3.4) and (3.5).

$$M = \min \begin{bmatrix} \frac{D_{\text{cri}}}{D_X} \\ \frac{D_{\text{cri}}}{D_Y} \\ \frac{D_{\text{cri}}}{D_Z} \end{bmatrix} \tag{3.4}$$

$$\begin{bmatrix} X'_{\text{ref}} \\ Y'_{\text{ref}} \\ Z'_{\text{ref}} \end{bmatrix} = M \begin{bmatrix} X_{\text{ref}} \\ Y_{\text{ref}} \\ Z_{\text{ref}} \end{bmatrix} \tag{3.5}$$

The block diagrams of the control system for the two operating modes are depicted in Figs. 3-4(a) and (b), respectively. For filtering the effect of instantaneous disturbances, the steady-state PWM duty cycle is smoothed by using Eqn. (3.6), where λ (= 0.995) and $(1 - \lambda)$ is the weight assigned to the cumulative average duty cycle $\bar{D}(k)$ and the newly sampled duty cycle $D(k)$, respectively.

$$\bar{D}(k) = \lambda \bar{D}(k-1) + (1-\lambda) D(k) \tag{3.6}$$

3 Implementation of LED Driver and Color Control System

The proposed RGB driver system, shown in Fig. 3-5, consists of a constant-current (as programmed by R_{cs}) buck converter implemented using LM3406 (from Texas Instruments), a dspic33fj-series DSP (from Microchip), an RGB color sensor

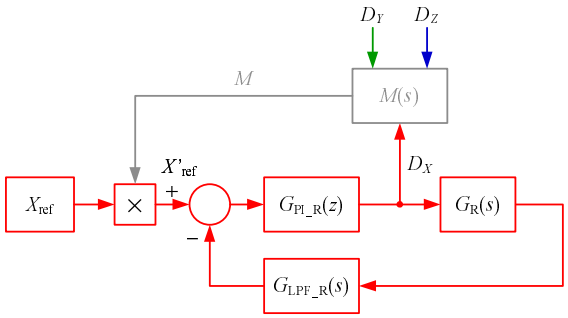

(a)

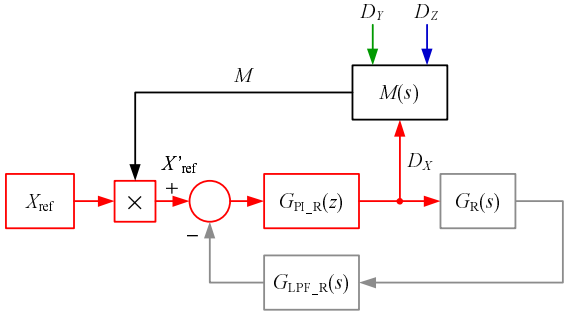

(b)

Figure 3-4: (a) Block diagram of the control system for Mode I: $D < D_{\mathrm{cri}}$. (b) Block diagram of the control system for Mode II: $D \geq D_{\mathrm{cri}}$.

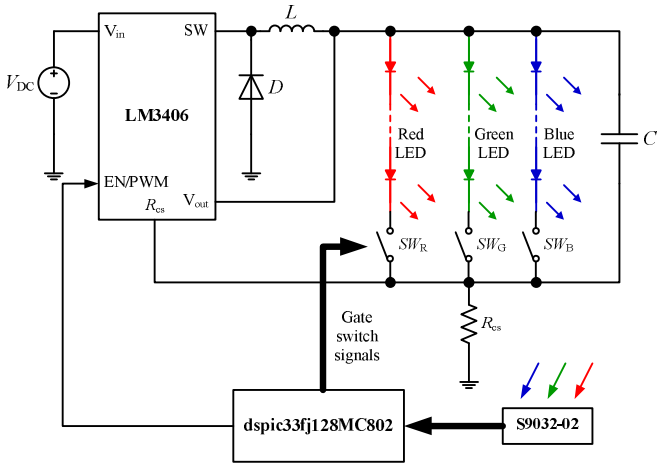

Figure 3-5: Schematic of the proposed color-sequential RGB driver system with color-sensing feedback control.

S9032-02 (from Hamamatsu Photonics), and an RGB LED module. As the system starts up, the DSP "enables" the buck converter with a PWM signal. The LED

branches are turned on and off by the switching signal produced by the DSP. The switching signal's frequency is selected to be 900 Hz so that each LED branch is turned on and off at a frequency of 300 Hz in order to avoid flickering. The luminance signal of the active branch is sensed by the RGB color sensor, and subsequently digitized by an ADC module and processed by a digital Kalman filter in the DSP. The reason for using a Kalman filter is to minimize the sensing error due to the decaying luminance from the ageing LEDs. The sampled luminance signal is further processed by a digital PID controller in the DSP, and the output is used to compute the necessary PWM duty cycle for each LED branch.

The flowchart shown in Fig. 3-6 summarizes the operation of the proposed color control method. The color point of the RGB LED is mainly regulated using a PID controller. Periodic checkpoints are inserted and tracked by a timer for performing regular checks on the PWM duty cycles used to drive the primary-color LEDs. The time interval between two periodic checks is assumed to be sufficiently long such that the sampled PWM duty cycles are steady-state values. When the PWM duty cycle(s) of one or more of the primary-color LEDs $\bar{D}_i(k)(i = X, Y, Z)$ exceeds the critical duty cycle D_{cri}, the minimum multiplier gain $M = \min[D_{\text{cri}}/\bar{D}_i(k)]$ is computed and used to update the reference tristimulus values according to Eqn. (3.5).

In the simplest design, D_{cri} can be set as a constant value. However, due to the different ageing rates of the red, green, and blue LED, it is difficult to find a suitable value that applies to all of them. For example, if D_{cri} is set far less than unity, the system will enter into Mode II's operation prematurely and cause the total luminance of the RGB LED to decrease. On the contrary, if D_{cri} is set too close to unity, the PWM duty cycle will reach unity very soon after which the color point of the RGB LED will become uncontrollable. Instead of setting D_{cri} to a constant value, the

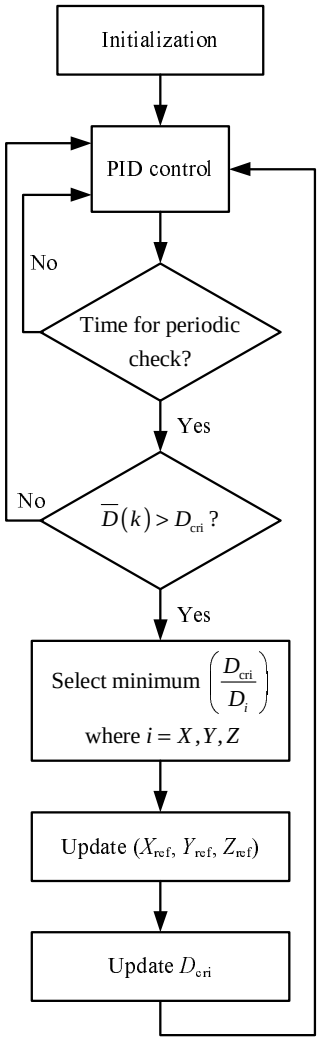

Figure 3-6: Flowchart of the proposed color control algorithm.

proposed system is designed to compute a new critical duty cycle D'_{cri} for each of the primary-color LEDs based on their duty cycle changes since the last periodic check, $(\bar{D}_i(k) - D_{\text{cri}})$, as given by Eqn. (3.7), where $i = X, Y, Z$. For more controllability, a user-defined margin w (≥ 1) can be included to account for the fluctuation in the ageing rate between two check periods. This allows the control algorithm to learn the individual ageing rates of the red, green, and blue LED and set their critical duty cycles adaptively.

$$D'_{\mathrm{cri}} = 1 - w \cdot (\bar{D}_i(k) - D_{\mathrm{cri}}) \tag{3.7}$$

After the reference tristimulus values and critical duty cycles are updated, the system returns control to the PID controller which regulates the color point of the RGB LED by tracking the new reference tristimulus values. This continues until the next periodic checkpoint is reached.

4 Experimental Verification

To demonstrate the ability of the proposed method to perform color-point regulation on aged LEDs, three primary-color LEDs are aged by subjecting them to repetitive current stress cycles with the test conditions listed in Table I. The luminance curves for red, green, and blue LED are plotted in Figs. 3-13(a)–(c). In general, the luminance of all three primary-color LEDs decreases as they are aged. Fig. 3-13 shows that the three types of LEDs have different decay rates although they are subjected to the same accelerated ageing test conditions. Hence, closed-loop regulation is necessary to maintain the color point constant at the desired value. It has been discussed in Section 1 that optical-sensor-based control is preferred as it enables a real-time monitoring and control of the luminance of the primary-color LEDs.

4.1 Details On Hardware Setup

The power stage of the RGB LED driver shown in Fig. 3-7 is similar to the power stage of the VBL current driver discussed in Chapter 2. The only difference is the removal of the switches($\mathrm{Sw}_1, \mathrm{Sw}_2 \mathrm{and} \mathrm{Sw}_3$). The current sensing resistor is changed in order to be consistent with this new design. The switches ,$\mathrm{Sw}_\mathrm{R}, \mathrm{Sw}_\mathrm{G} \mathrm{and} \mathrm{Sw}_\mathrm{B}$,

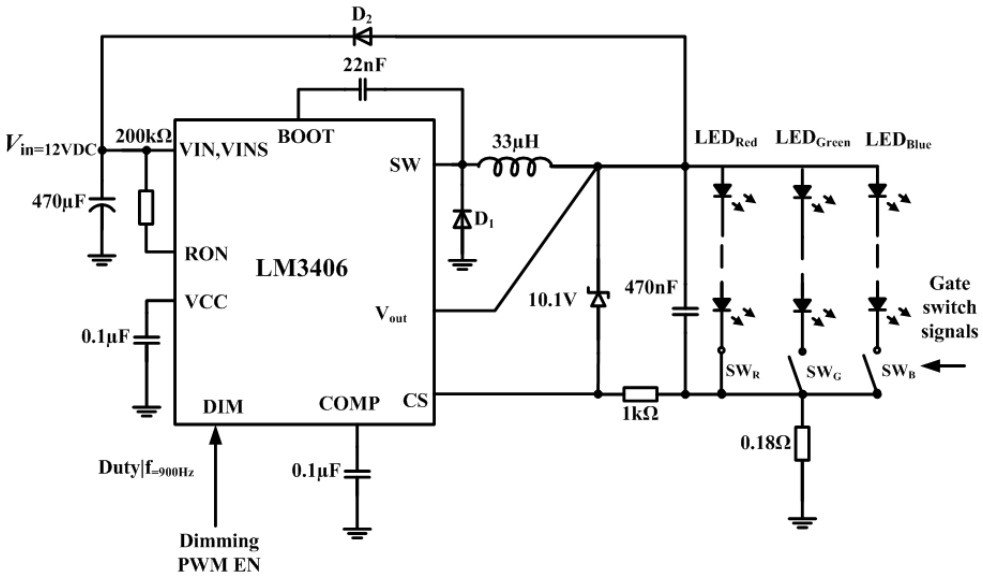

Figure 3-7: Schematic of power stage of high power RGB LED driver.

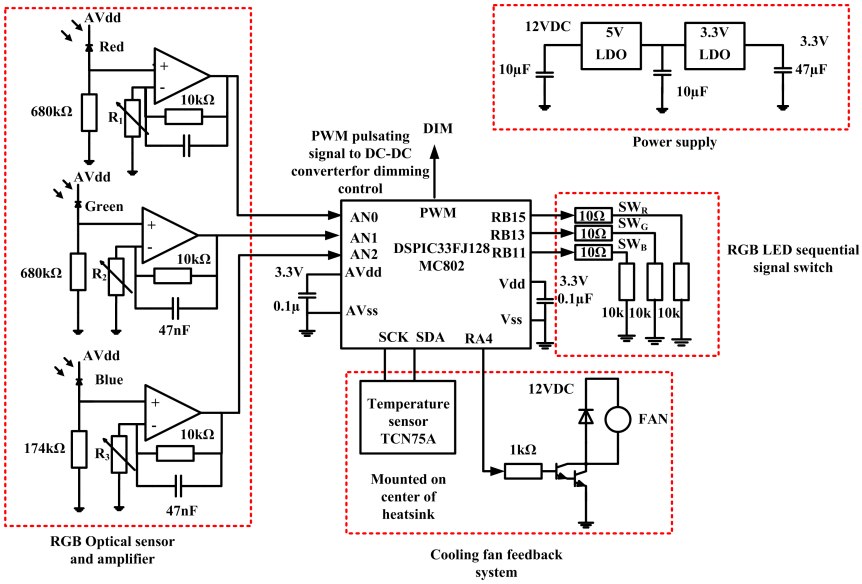

Figure 3-8: Schematic of the dsp controller of high power RGB LED driver.

have the same function as before, i.e. provides sequential color switching. The DIM pin is used to receive the PWM signal to control the light intensity of each color phase. The optical output of the RGB LED is sensed by the reversed-connected optical sensor as shown in Fig. 3-8. The sensed signal is then amplified by the non-

inverting amplifier with a $2\ \mathrm{kHz}$ band widthlow pass filter. The gain can be adjusted by using the adjustable resistor. The amplified signals are converted to digital signal by the internal ADC conversion module.

The digital controller can obtain information about the optical intensity signal from the sensed signal, and adjust the dimming duty cycle to keep it regulated at the reference value. In General, the dimming duty cycle will increase once the RGB LED begin to age.

The optical signal intensity is sampled at $300\ \mathrm{Hz}$, which means one sample will be collected per color phase. Hence, the intensity of each color is monitored independently. The sampled optical signal can be calculated by the Eqn.(3.8). First, the output flux , $f(\Phi_i)$ will be converted to a sensed voltage ($V_{sens,i}$). it is then amplified by the amplifier with a gain of G_i and digitized by the internal ADC module. Finally, the average flux can be calculated by multiplying $V_(adc, i)$ with the dimming duty cycle , $D_{dimming,i}$. Table 3.1 shows the ADC parameters. The resulting signal will be processed by the PI compensator for regulating the color emitted by each color phase. The PI parameters used for the feedback controller are tuned by the Ziegler-Nichols's closed loop Tunning method. They are shown in Table 3.2.

$$\begin{aligned} V_{sens,i} &= f(\Phi_i) \\ V_(adc, i) &= V_{sens,i} \times G_i \\ \overline{\Phi}_i &= V_(adc, i) \times \overline{D}_{dimming,i} \end{aligned} \tag{3.8}$$

where i=R,G or B

Fig. 3-9shows the schematic of the experimental setup of the proposed system. The RGB LED is mounted on a heat sink and covered with a diffuser. The function of the diffuser is to evenly mix the RGB color. On the surface of the diffuser, a RGB color sensor is mounted to monitor the intensities of the three primary color.s

Table 3.1: Sampling and ADC parameters .

Parameter	
ADC resolution	10 bits
Conversion time	125 kSPS
Sampling frequency	300 Hz

Table 3.2: Tuned PI parameters based on the Ziegler-Nichols's Tunning closed loop method.

Parameter	P	I
R	0.001485	0.002578
G	0.002053612	0.006417538
B	0.028294	0.055262

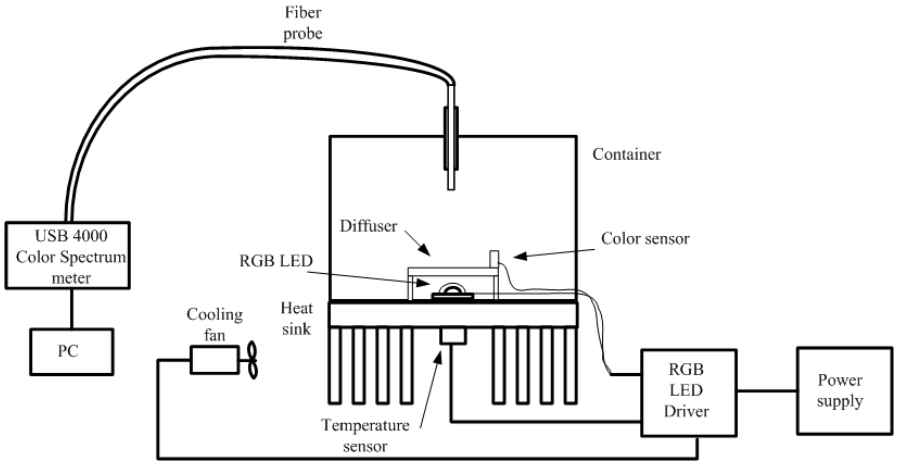

Figure 3-9: Schemtaic of experiment setup .

A temperature sensor is mounted at the center of the bottom side of the heat sink close to the RGB LED. This position is naturally more sensitive to the changes in the heat sink's temperature as affected by the heat source , i.e. the RGB LED. A temperature feedback cooling fan system is also now installed next to the heat sink in order to maintain the heat sink's temperature constant. The Ocean Optics USB 4000 color spectrometer is used to collect the optical information which is used for

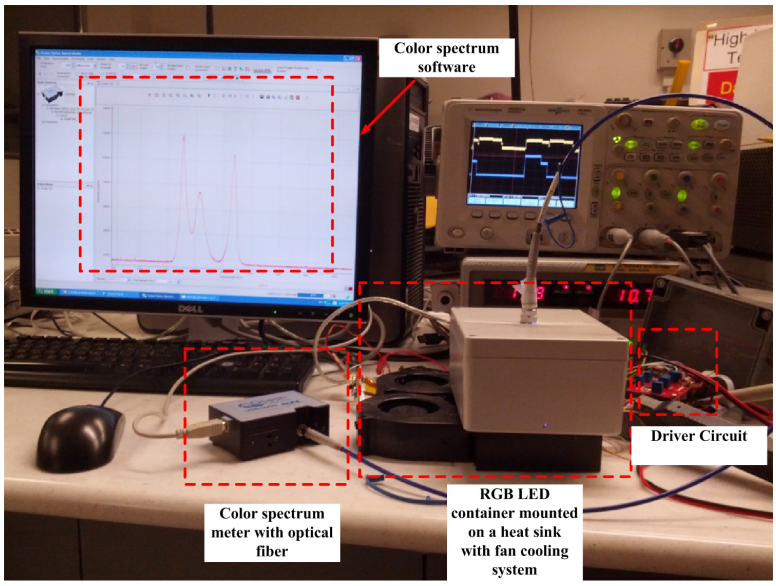

Figure 3-10: Experiment setup high power RGB LED driver.

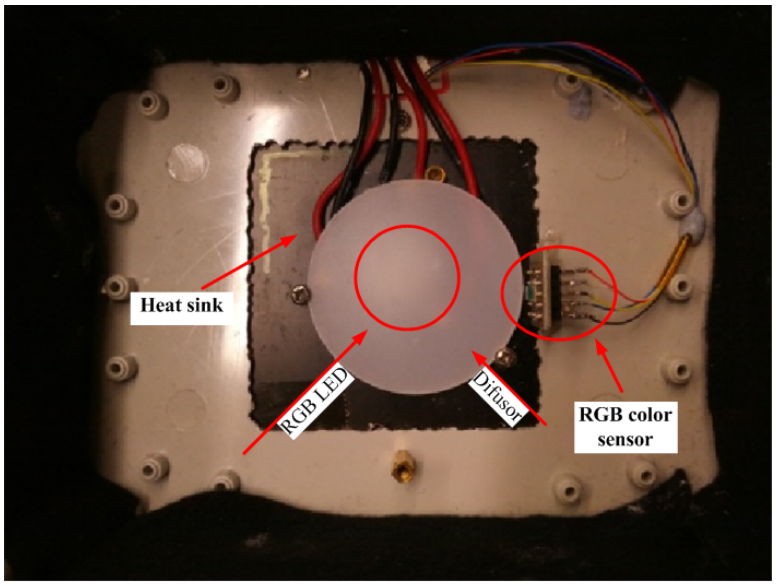

Figure 3-11: Experiment setup inner side of RGB LED lamp .

calibration and analysis of the RGB LED spectrum.. Fig. 3-10 and Fig. 3-11 show the actual laboratory setup .

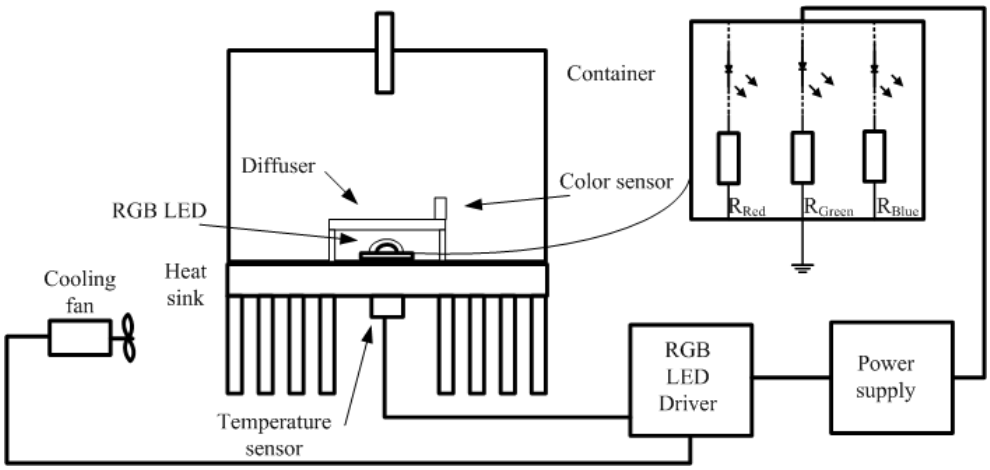

Figure 3-12: Setup of RGB LED over DC ageing with constant heatsink temperature control.

4.2 Accelerated Ageing Test

Fig. 3-12 shows the repetitive accelerated ageing test is conducted by applying high DC current to the RGB LED. Each primary-color LED string is connected in series with a power resistor to stabilize the DC current supplied from the power supply. The power resistors are mounted on heat sink for cooling during the test.

4.3 Result

Table 3.3: Operating Conditions for Accelerated Ageing Test on RGB LED Module Samples.

Parameter	Value
Heat sink's thermal resistance	1.1°C/W
Heat sink's temperature	60°C
RGB LED (Sample 1)	Lamina NT-43F0-0424
RGB LED (Sample 2)	LedEngin LZ4-00MC00
Current (DC)	1.5 A (for Sample 1)
	2.0 A (for Sample 2)

Fig. 3-14 shows the trends of duty cycle changes for the three primary-color LEDs when color control is performed by the conventional method and the proposed

Table 3.4: Main Components and Operating Conditions of the Proposed RGB Driver System.

Parameter	Value
Heat sink's thermal resistance	1.1°C/W
Heat sink's temperature	30°C
Maximum average current per LED	350 mA
RGB color sensor	Hamamatsu S9032-02
DSP	dspic33fj128MC802
Controller for buck converter	LM3406
Spectrometer	Ocean Optics USB4000
Lux-meter	TES-1336A

method with threshold current detection. As indicated by the degree of duty cycle increase, the blue LED is found to exhibit the fastest decay among the three primary-color LEDs. With conventional color control, in the absence of threshold current detection, the duty cycle applied to the blue LED keeps increasing until it saturates at the maximum duty cycle, beyond which color control is no longer possible. On the contrary, as the ageing time exceeds about 22 minutes, the proposed control method has prevented the saturation of duty cycle by detecting the threshold current and maintains the duty cycle applied to the blue LED below the maximum value with some small variations due to the adaptive setting of the threshold current. Since the luminance decay rates of the red and green LEDs are slower compared to the blue LED as shown in Fig. 3-14, their duty cycles are monotonically decreased by the algorithm in order to keep the color point constant at the desired value.

Fig. 3-15 compares the measured uniform chromaticity coordinates (u, v) resulting from the conventional method and the proposed method with threshold current detection. Due to the saturation of the duty cycle applied to the blue LED, the chromaticity coordinates obtained with conventional color control are found to deviate significantly from the desired values after the duty cycle has saturated and closed-

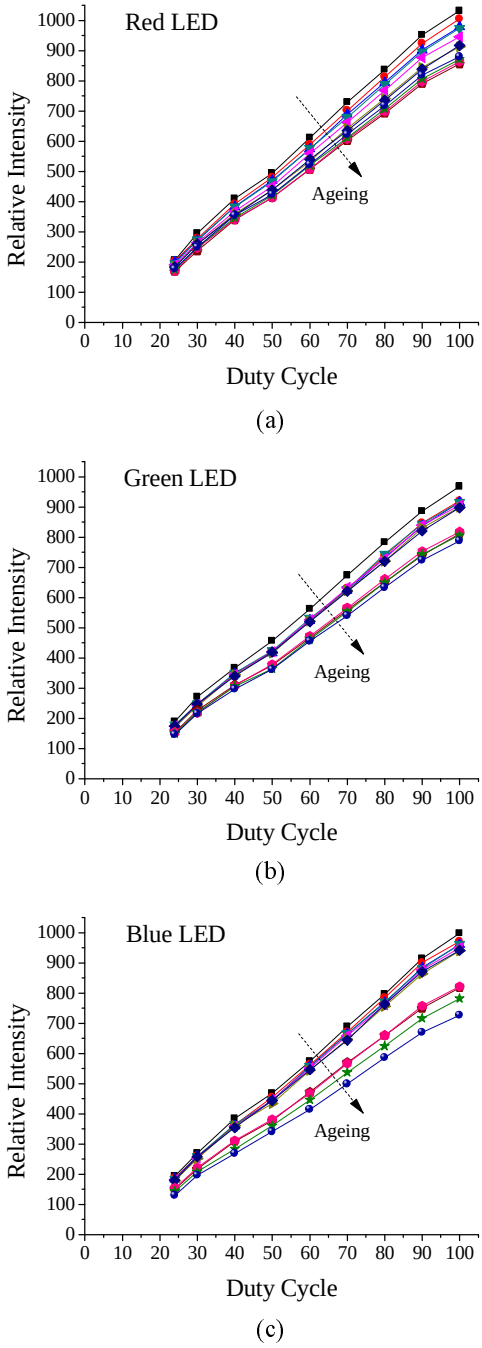

Figure 3-13: Measured luminance decay of (a) red, (b) green, (c) blue LED (of Lamina NT-43F0-0424 RGB LED module) with ageing.

loop feedback control is no longer operative. When the proposed color control method is employed, the duty cycle applied to the blue LED is constantly monitored

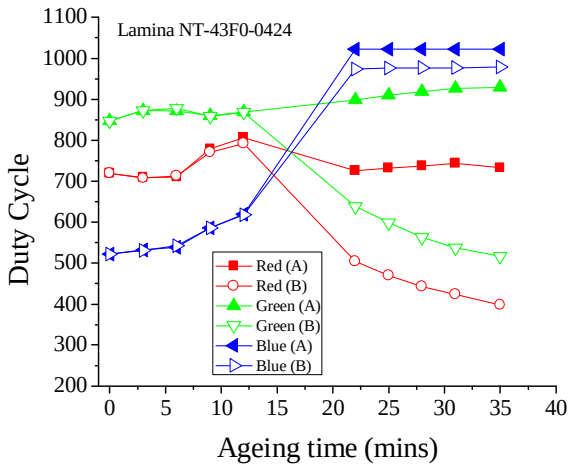

Figure 3-14: Duty cycle changes for red, green, and blue LED (of Lamina NT-43F0-0424 RGB LED module) as a function of ageing time under two color control methods. "A" and "B" refers to the conventional method and the proposed method, respectively.

and maintained at the critical value corresponding to the threshold current, hence the closed-loop feedback control remains active and acts to regulate the chromaticity co-ordinates at the desired values. In order to hold the duty cycle at the critical value, the reference tristimulus value of the blue LED will be continuously decreased by the algorithm as it is further aged, and the references of the red and green LEDs will be scaled proportionally in order to keep the color point constant. This process causes the overall luminance of the RGB LED to decrease, as shown in Fig. 3-16, for the purpose of maintaining the color quality of the LED system. It can be seen that, although human eyes are not sensitive to blue color, the fact that it decays at the highest rate during ageing and cause the other two colors and the overall illuminance to decrease in order to maintain the color point constant, makes the fast ageing of blue LED a case deserving further studies.

In order to check if the same observation also occurs to RGB LEDs made by other manufacturers, the accelerated ageing test was performed on another RGB LED sample – LedEngin LZ4-00MC00. For this RGB LED sample, the green LED is found to exhibit the fastest decay among the three primary-color LEDs, as shown

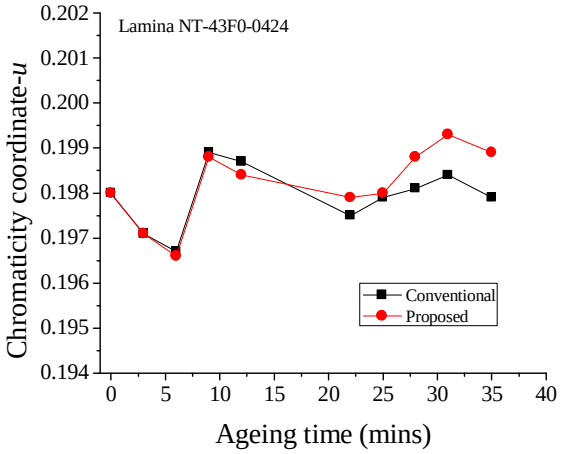

(a)

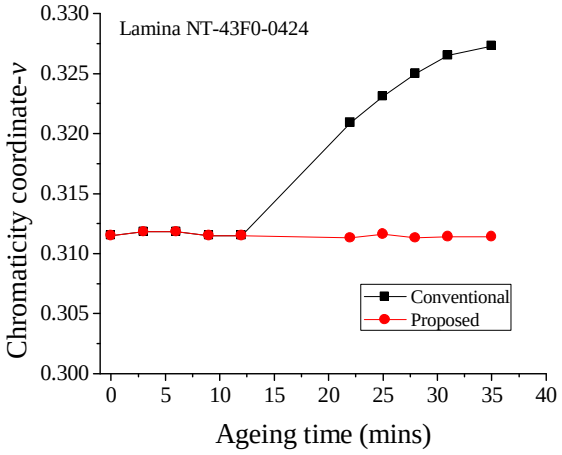

(b)

Figure 3-15: Comparison of measured CIE-1960 uniform chromaticity coordinates (u, v) of Lamina NT-43F0-0424 RGB LED module when its color is controlled by the conventional method and the proposed method.

in Fig. 3-17. With the proposed control method, the duty cycle applied to the green LED is maintained at the critical value while those applied to the red and blue LEDs are monotonically decreased in order to keep the color point constant. A comparison of the measured chromaticity coordinates (u, v) of this RGB LED sample under the actions of the two color control methods is shown in Fig. 3-18, where a significant color deviation occurs after the green LED has reached the maximum duty cycle

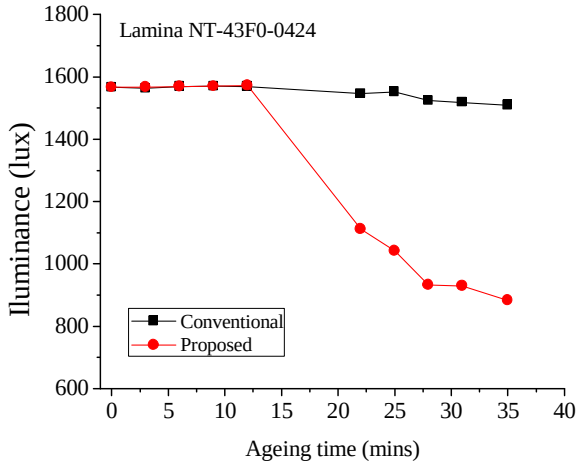

Figure 3-16: Comparison of illuminance change of Lamina NT-43F0-0424 RGB LED module when its color is controlled by the conventional method and the proposed method.

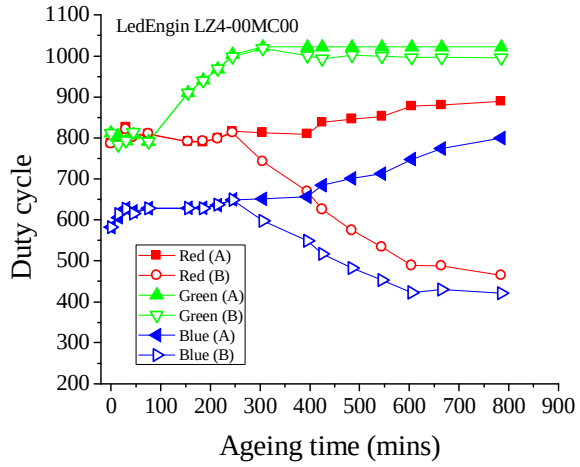

Figure 3-17: Duty cycle changes for red, green, and blue LED (of LedEngin LZ4-00MC00 RGB LED module) as a function of ageing time under two color control methods. "A" and "B" refers to the conventional method and the proposed method, respectively.

when the conventional control method is used. Finally, the luminance changes of the RGB LED sample under the actions of the two color control methods are shown in Fig. 3-19. Since human eyes are sensitive to green color, the inability of the conventionally controlled system to further increase the driving current for the green LED is responsible for the rapid decrease of luminance after the green LED has reached the maximum duty cycle. In this case, the two color control methods are not

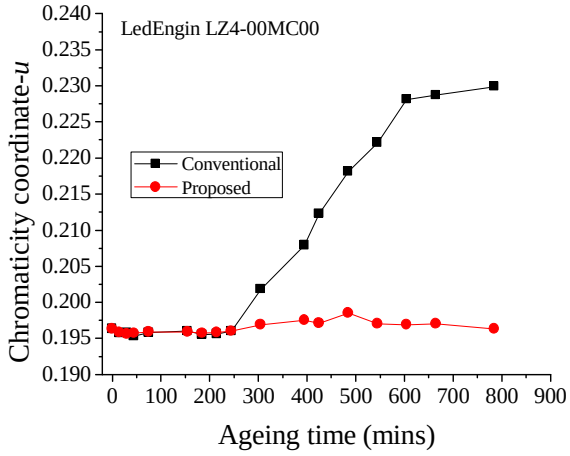

(a)

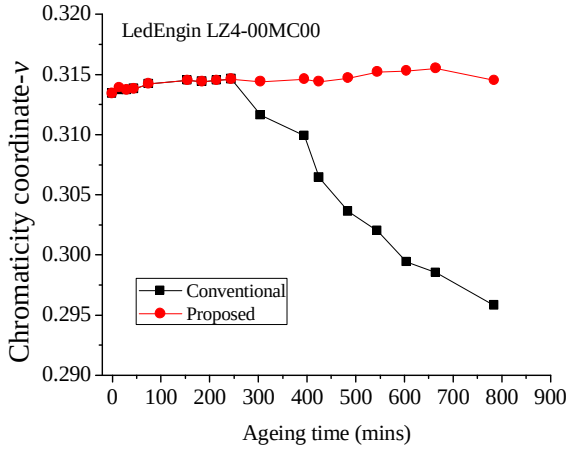

(b)

Figure 3-18: Comparison of measured CIE-1960 uniform chromaticity coordinates (u, v) of LedEngin LZ4-00MC00 RGB LED module when its color is controlled by the conventional method and the proposed method.

significantly different in their effects on the overall luminance of the RGB LED.

Comparing the two sets of experimental data taken from two RGB LED samples, it is clear that RGB LEDs made by different manufacturers can show very different levels of tolerance to the ageing test, *i.e.* the Lamina sample entered into Mode II's operation after 12 mins and the LedEngin sample only did so after 245 mins when stressed with 33% larger DC current. Since both blue and green LEDs are made

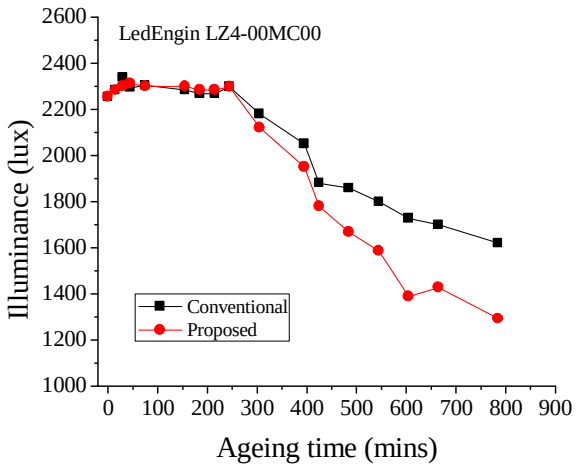

Figure 3-19: Comparison of illuminance change of LedEngin LZ4-00MC00 RGB LED module when its color is controlled by the conventional method and the proposed method.

from indium gallium nitride (InGaN), the results may have indicated to us, although not conclusively, that this family of LEDs tends to age faster than red LEDs and improvement in their durability should desirably be pursued. Lastly, while the RGB LED system controlled by the conventional method should be replaced when color deviation begins to occurs (at 12 mins and 245 mins for the Lamina and LedEngin sample, respectively), another system controlled by the proposed method will have a useful lifetime extended to nearly two times as long (to 23 mins and 550 mins for the Lamina and LedEngin sample, respectively). In the latter case, since color deviation does not occur, the useful lifetime of the RGB LED is assumed to have reached the end when its luminance has decreased to 70% of its initial value.

5 Conclusion

An optical-sensor-based color control method for maintaining the white color point of RGB LED existing in all ageing states was proposed. The method is based on the concept of threshold current detection which is aimed to prevent the saturation

of duty cycle when the RGB LED is in its late ageing state, so that the color quality of the LED system can be continuously maintained throughout its service lifetime. The design of the color control method was discussed and verified experimentally by subjecting RGB LED samples to accelerated ageing tests and measuring their color changes. The verification was done on single RGB LED module which is appropriate for use in smart phones, RGB LED backlight for LCD monitors or small LED projectors. With further development, the algorithm can be applied to multi-projector system that contains a networking system for enabling communication between all projectors. This setup can be used to provide a global brightness and color control based on the information sharing between the networked projectors.

Chapter 4

Conclusion

1 Contributions of the Thesis

The contributions of the thesis mainly consist of two parts. In the first part, a micro-controller based implementation of the variable bi-level current driving method was proposed. The overall system employs only one power converter for cost saving and compactness, where the primary-color LEDs are driven in a time sequential manner at a cyclic frequency higher than the flicker threshold of human eyes. With the variable bi-level current driving approach, the dc luminous output characteristic of each primary-color LED is represented by a piecewise-linear approximation and the method for selecting the required current levels was demonstrated. As each primary-color LED can now be dimmed by varying the dimming duty cycle or current level, or both, it was shown that the additional flexibility in dimming with variable bi-level current driving method can theoretically lead to a significant improvement in the color resolution of the resulting RGB lighting system. Besides, it has also been shown that the use of variable bi-level current driving method has led to a significant improvement in the luminous efficacy of the RGB LED.

In the second part, the color control system for RGB LED was studied in detail. A new color control algorithm was proposed to compensate for the color drift effect of ageing RGB LED. In this study, it was found that the ageing process of the red, green, and blue LED is nonlinear with time and their ageing rates are different from each other. Hence, an optical sensor based feedback control system was proposed in order to monitor and adjust the color of RGB LED in real time. The proposed algorithm is designed to operate in two modes. Before the RGB LED has aged significantly and the dimming duty cycle has not reached the threshold value, the color of the RGB LED is controlled by adjusting the dimming duty cycle of each primary-color LED. At the late ageing state of the RGB LED where the dimming duty cycle of one or more primary-color LED has reached the threshold value, the reference tri-stimulus values of the remaining LEDs are adjusted in order to keep the color point constant. To verify the effectiveness of the proposed color control algorithm, RGB LEDs made by different manufacturers were subjected to accelerated lifetime test and their color point was measured as a function of ageing time. It was found that by adopting the proposed color control algorithm, the color stability of the RGB LED can be maintained even when the LED is deeply aged. It was shown that, compared to the conventional color control method which can subject the RGB LED to a premature end-of-life, the useful lifetime of the RGB LED controlled with the proposed color control algorithm can be significantly extended.

2 Future Works

Although the experimental verification of the proposed RGB color control system was performed on single RGB LED module, which is appropriate for use in smart phones, RGB LED backlight for LCD monitors or small LED projectors, it

is believed that, with further development, the algorithm can be applied to multi-projector system that contains a networking system for enabling communication between all projectors. This setup can be used to provide a global brightness and color control based on the information sharing between the networked projector. Besides, although PWM driving is used for dimming in the proposed color control system, a further adaptation of the system for dimming with the variable bi-level current driving method should be pursued for improving the overall luminous efficacy of the RGB LED system.

References

[1] L. L. incorporated, "atLas^{TM} series LED Light engines," datasheet, 2008.

[2] G.Hoffmann, "CIE Color Space," http://www.fho-emden.de/~hoffmann, 2010, [Online; accessed 20-July-2012].

[3] C.-C. Chen, C.-Y. Wu, P.-C. Lu, Y.-M. Chen, and T.-F. Wu, "Sequential Color LED Back-Light Driving System for LCD Panels," *IEEE Power Electronics and Motion Control.Conf.(IPEMC 2006)*, vol. 1, pp. 1–5, Aug. 2006.

[4] TI, "pico DLP," http://www.ti.com/analog/docs/dlptoplevel.tsp?sectionId=622&tabId=2441&familyId=1743, [Online; accessed 1-June-2012].

[5] S. M. Moon, S. W. Chae, and J. S. Kwak, "High-temperature electro-optical degradation of DC-Aged InGaN based high power GaN LEDs," in *Device Research Conference, 2009. DRC 2009*, June 2009, pp. 95 –96.

[6] C.-Y. Hsieh and K.-H. Chen, "Boost DC-DC Converter With Fast Reference Tracking (FRT) and Charge-Recycling (CR) Techniques for High-Efficiency and Low-Cost LED Driver," *Solid-State Circuits, IEEE Journal of*, vol. 44, no. 9, pp. 2568 –2580, Sept. 2009.

[7] N. Holonyak and S. F. Bevacqua, "COHERENT (VISIBLE) LIGHT EMISSION FROM Ga(As1-xPx) JUNCTIONS," *Applied Physics Letters*, vol. 1, no. 4, pp. 82 –83, Dec. 1962.

[8] C. P. Kuo, R. M. Fletcher, T. D. Osentowski, M. C. Lardizabal, M. G. Craford, and V. M. Robbins, "High performance AlGaInP visible light emitting diodes," *Applied Physics Letters*, vol. 57, no. 27, pp. 2937 –2939, Dec. 1990.

[9] S. Nakamura, "High-power InGaN/AlGaN double-heterostructure blue-light-emitting diodes," in *Electron Devices Meeting, 1994. IEDM '94. Technical Digest., International*, Dec. 1994, pp. 567 –570.

[10] R. Mueller-Mach, G. Mueller, M. Krames, and T. Trottier, "High-power phosphor-converted light-emitting diodes based on III-Nitrides," *Selected Topics in Quantum Electronics, IEEE Journal of*, vol. 8, no. 2, pp. 339 –345, Mar.-Apr. 2002.

[11] X. QU, "Development and Design of Light-emitting-diode (LED) Lighting Power Supplies," Ph.D. dissertation, The Hong Kong Polytechnic University, Nov. 2009.

[12] L. Wai-keung, "On driving techniques for high-brightness light-emitting diodes," Master's thesis, The Hong Kong Polytechnic University, Nov. 2009.

[13] Adobe, "Adobe RGB 1998," http://www.adobe.com/digitalimag/pdfs/AdobeRGB1998.pdf, 1998, [Online; accessed 22-June-2012].

[14] H.-J. Chiu, Y.-K. Lo, T.-P. Lee, S.-C. Mou, and H.-M. Huang, "Design of an RGB LED Backlight Circuit for Liquid Crystal Display Panels," *Industrial Electronics, IEEE Transactions on*, vol. 56, no. 7, pp. 2793 –2795, July 2009.

[15] Y.-H. Liu, Z.-Z. Yang, and S.-C. Wang, "A novel sequential-color RGB-LED backlight driving system with local dimming control and dynamic bus voltage regulation," *Consumer Electronics, IEEE Transactions on*, vol. 56, no. 4, pp. 2445 –2452, Nov. 2010.

[16] S. C. Shin, Y. Jung, T.-J. Ahn, S. S. Jeong, S.-G. Lee, and K.-Y. Choi, "The Compact Systems Design Based on DMD and the Straight Line 2-Channel LED for a Mobile Embedded Pico Projector," *Display Technology, Journal of*, vol. 8, no. 4, pp. 219 –224, Apr. 2012.

[17] J. Yan, Z. Shang, and J. Chen, "Investigation on the aging characteristics of high-power white LEDs under different stresses," in *Communications and Photonics Conference and Exhibition (ACP), 2009 Asia*, Nov. 2009, pp. 1 –2.

[18] Y.-C. Hsu, Y.-K. Lin, M.-H. Chen, C.-C. Tsai, J.-H. Kuang, S.-B. Huang, H.-L. Hu, Y.-I. Su, and W.-H. Cheng, "Failure Mechanisms Associated With Lens Shape of High-Power LED Modules in Aging Test," *Electron Devices, IEEE Transactions on*, vol. 55, no. 2, pp. 689 –694, Feb. 2008.

[19] C.-C. Tsai, M.-H. Chen, Y.-C. Huang, Y.-C. Hsu, Y.-T. Lo, Y.-J. Lin, J.-H. Kuang, S.-B. Huang, H.-L. Hu, Y.-I. Su, and W.-H. Cheng, "Decay Mechanisms of Radiation Pattern and Optical Spectrum of High-Power LED Modules in Aging Test," *Selected Topics in Quantum Electronics, IEEE Journal of*, vol. 15, no. 4, pp. 1156 –1162, July-Aug. 2009.

[20] G. Meneghesso, S. Levada, R. Pierobon, F. Rampazzo, E. Zanoni, A. Cavallini, A. Castaldini, G. Scamarcio, S. Du, and I. Eliashevich, "Degradation mechanisms of GaN-based LEDs after accelerated DC current aging," in *Electron Devices Meeting, 2002. IEDM '02. Digest. International*, 2002, pp. 103 – 106.

[21] M. Meneghini, L.-R. Trevisanello, U. Zehnder, T. Zahner, U. Strauss, G. Meneghesso, and E. Zanoni, "High-Temperature Degradation of GaN LEDs Related to Passivation," *Electron Devices, IEEE Transactions on*, vol. 53, no. 12, pp. 2981 –2987, Dec. 2006.

[22] F.-J. S. Subramanian Muthu and M. Pashley, "Red, Green, and Blue LED based white light generation: Issues and control," *IEEE Industry Appl.Conf. IAS 2002*, vol. 1, pp. 327 – 333, Oct. 2002.

[23] S. Koh, W. Van Driel, and G. Zhang, "Degradation of epoxy lens materials in LED systems," in *Thermal, Mechanical and Multi-Physics Simulation and Experiments in Microelectronics and Microsystems (EuroSimE), 2011 12th International Conference on*, Apr. 2011, pp. 1/5 –5/5.

[24] S. Buso, G. Spiazzi, M. Meneghini, and G. Meneghesso, "Performance Degradation of High-Brightness Light Emitting Diodes Under DC and Pulsed Bias," *Device and Materials Reliability, IEEE Transactions on*, vol. 8, no. 2, pp. 312 –322, June 2008.

[25] G. Zhang, S. Feng, H. Deng, J. Li, Z. Zhou, and C. Guo, "Thermal stability evaluation of die attach for high brightness LEDs," in *Semiconductor Thermal Measurement and Management Symposium (SEMI-THERM), 2011 27th Annual IEEE*, Mar. 2011, pp. 305 –309.

[26] S. Muthu and J. Gaines, "Red, green and blue LED-based white light source: implementation challenges and control design," *IEEE Industry Appl.Conf. IAS 2003*, vol. 1, pp. 515 – 522, Oct. 2003.

[27] X. Qu, S.-C. Wong, and C. Tse, "Temperature Measurement Technique for Stabilizing the Light Output of RGB LED Lamps," *Instrumentation and Measurement, IEEE Transactions on*, vol. 59, no. 3, pp. 661 –670, Mar. 2010.

[28] M. Doshi and R. Zane, "Control of Solid-State Lamps Using a Multiphase Pulsewidth Modulation Technique," *Power Electronics, IEEE Transactions on*, vol. 25, no. 7, pp. 1894 –1904, July 2010.

[29] G. Carraro, "Solving high-voltage off-line HB-LED constantcurrent contro-circuit issues," in *Applied Power Electronics Conference, APEC 2007 - Twenty Second Annual IEEE*, Mar. 2007, pp. 1316 –1318.

[30] I.-H. Oh, "An analysis of current accuracies in peak and hysteretic current controlled power LED drivers," in *Applied Power Electronics Conference and Exposition, 2008. APEC 2008. Twenty-Third Annual IEEE*, Feb. 2008, pp. 572 –577.

[31] H. Pang and P. Bryan, "A stability issue with current mode control flyback converter driving LEDs," in *Power Electronics and Motion Control Conference, 2009. IPEMC '09. IEEE 6th International*, May 2009, pp. 1402 –1406.

[32] K. Loo, W.-K. Lun, S.-C. Tan, Y. Lai, and C. Tse, "On Driving Techniques for LEDs: Toward a Generalized Methodology," *Power Electronics, IEEE Transactions on*, vol. 24, no. 12, pp. 2967 –2976, Dec. 2009.

[33] S.-C. Tan, "General n-Level Driving Approach for Improving Electrical-to-Optical Energy-Conversion Efficiency of Fast-Response Saturable Lighting Devices," *Industrial Electronics, IEEE Transactions on*, vol. 57, no. 4, pp. 1342 –1353, Apr. 2010.

[34] S. Beczkowski and S. Munk-Nielsen, "LED spectral and power characteristics under hybrid PWM/AM dimming strategy," in *Energy Conversion Congress and Exposition (ECCE), 2010 IEEE*, Sept. 2010, pp. 731 –735.

[35] M. Doshi and R. Zane, "Digital Architecture for Driving Large LED Arrays with Dynamic Bus Voltage Regulation and Phase Shifted PWM," in *Applied Power Electronics Conference, APEC 2007 - Twenty Second Annual IEEE*, Mar. 2007, pp. 287 –293.

[36] C.-Y. Wu, T.-F. Wu, J.-R. Tsai, Y.-M. Chen, and C.-C. Chen, "Multistring LED Backlight Driving System for LCD Panels With Color Sequential Display and Area Control," *Industrial Electronics, IEEE Transactions on*, vol. 55, no. 10, pp. 3791 –3800, Oct. 2008.

[37] F.-J. Subramanian Muthu and M.-D. Pashley, "Red, Green, and Blue LEDs for White Light Illumination," *IEEE Trans. Quamtum Electronics. Selected topics*, vol. 8, no. 2, pp. 333–338, Aug. 2002.

[38] T. Sun and C. Wang, "Specially Designed Driver Circuits to Stabilize LED Light Output without a Photo-detector," *Power Electronics, IEEE Transactions on*, vol. PP, no. 99, p. 1, 2011.

[39] Y.-K. Lo, K.-H. Wu, K.-J. Pai, and H.-J. Chiu, "Design and Implementation of RGB LED Drivers for LCD Backlight Modules," *Industrial Electronics, IEEE Transactions on*, vol. 56, no. 12, pp. 4862 –4871, Dec. 2009.

[40] H.-J. Chiu and S.-J. Cheng, "LED Backlight Driving System for Large-Scale LCD Panels," *Industrial Electronics, IEEE Transactions on*, vol. 54, no. 5, pp. 2751 –2760, Oct. 2007.

[41] W.-K. Lun, K. Loo, S.-C. Tan, Y. Lai, and C. Tse, "Bilevel Current Driving Technique for LEDs," *Power Electronics, IEEE Transactions on*, vol. 24, no. 12, pp. 2920 –2932, Dec. 2009.

[42] D. Sheet, "1.5 a constant current buck regulator for driving high power LED," *National Semiconductor*, Aug. 2010.

[43] C.-C. Chen, C.-Y. Wu, Y.-M. Chen, and T.-F. Wu, "Sequential Color LED Backlight Driving System for LCD Panels," *Power Electronics, IEEE Transactions on*, vol. 22, no. 3, pp. 919 –925, May 2007.

[44] J. Hasan, D. H. Nguyen, and S. Ang, "A RGB-driver for LED display panels," in *Applied Power Electronics Conference and Exposition (APEC), 2010 Twenty-Fifth Annual IEEE*, Feb. 2010, pp. 750 –754.

[45] T.-W. Lee, J.-H. Lee, C.-G. Kim, and S.-H. Kang, "An optical feedback system for local dimming backlight with RGB LEDs," *Consumer Electronics, IEEE Transactions on*, vol. 55, no. 4, pp. 2178 –2183, Nov. 2009.

[46] E. Bhasker, P. Sinha, and A. Majumder, "Asynchronous Distributed Calibration for Scalable and Reconfigurable Multi-Projector Displays," *Visualization and Computer Graphics, IEEE Transactions on*, vol. 12, no. 5, pp. 1101 –1108, Sept.-Oct. 2006.

[47] W.-L. Chen, C.-S. Wu, C.-Y. Chen, S.-C. Cheng, and C.-H. Tsai, "Development of an autostereoscopic display system using projectors array," in *3DTV-Conference: The True Vision - Capture, Transmission and Display of 3D Video (3DTV-CON), 2010*, June 2010, pp. 1 –4.

[48] A. Lathuiliere, F. Marzani, and Y. Voisin, "Colour 3D system characterization," in *IEEE Industrial Electronics, IECON 2006 - 32nd Annual Conference on*, Nov. 2006, pp. 3232 –3237.

[49] B. Sajadi, M. Lazarov, M. Gopi, and A. Majumder, "Color Seamlessness in Multi-Projector Displays Using Constrained Gamut Morphing," *Visualization and Computer Graphics, IEEE Transactions on*, vol. 15, no. 6, pp. 1317 –1326, Nov.-Dec. 2009.

[50] A. Majumder and R. Stevens, "Color nonuniformity in projection-based displays: analysis and solutions," *Visualization and Computer Graphics, IEEE Transactions on*, vol. 10, no. 2, pp. 177 –188, Mar.-Apr. 2004.

[51] A. Majumder, R. Brown, and H. El-Ghoroury, "Display gamut reshaping for color emulation and balancing," in *Computer Vision and Pattern Recognition Workshops (CVPRW), 2010 IEEE Computer Society Conference on*, June 2010, pp. 17 –24.

[52] X.-J. Yu, Y. Ho, L. Tan, H.-C. Huang, and H.-S. Kwok, "LED-Based Projection Systems," *Display Technology, Journal of*, vol. 3, no. 3, pp. 295 –303, Sept. 2007.

[53] J. Garcia, M. Dalla-Costa, J. Cardesin, J. Alonso, and M. Rico-Secades, "Dimming of High-Brightness LEDs by Means of Luminous Flux Thermal Estimation," *Power Electronics, IEEE Transactions on*, vol. 24, no. 4, pp. 1107 –1114, Apr. 2009.

[54] S. Ng, K. Loo, S. Ip, Y. Lai, C. Tse, and K. Mok, "Sequential Variable Bilevel Driving Approach Suitable for Use in High-Color-Precision LED Display Panels," *Industrial Electronics, IEEE Transactions on*, vol. 59, no. 12, pp. 4637 –4645, dec. 2012.